

**The role of *FMT* and *FIS1A* in mitochondrial morphology  
and salt stress in *Arabidopsis thaliana***

**Inaugural-Dissertation**

**zur  
Erlangung des Doktorgrades  
der Mathematisch-Naturwissenschaftlichen Fakultät  
der Universität zu Köln**

**vorgelegt von  
Alexandra Ralevski**

**Köln, October 2016**

Berichterstatter:

Prof. Dr. Jens Brüning  
Prof. Dr. Thomas Langer  
Prof. Dr. Tamas Horvath

Prüfungsvorsitzender:

Prof. Dr. Peter Kloppenburg

Tag der mündlichen Prüfung:

28 Oct 2016

## Table of Contents

<b>Abbreviations</b> .....	<b>III</b>
<b>Nomenclature</b> .....	<b>III</b>
<b>List of figures</b> .....	<b>IV</b>
<b>Abstract</b> .....	<b>V</b>
<b>Zusammenfassung</b> .....	<b>VI</b>
<b>1. Introduction</b> .....	<b>1</b>
1.1 Effects of soil salinity on agriculture .....	1
1.2 Effects of soil salinity on plants .....	2
1.3 Plant responses to salinity .....	3
1.4 Mitochondrial response to stress .....	4
1.4.1 The hypersensitive response and programmed cell death .....	4
1.4.2 The SOS Pathway.....	5
1.4.3 Reorganization of Root System Architecture and salt-avoidance tropism .....	6
1.5 Mitochondrial clustering in response to stress .....	8
1.6 The FMT/CLU and FIS1A genes in eukaryotes .....	9
1.7 Thesis aims .....	12
<b>2. Material and Methods</b> .....	<b>13</b>
2.1 Material .....	13
2.1.1. Antibiotics .....	13
2.1.2 Bacterial strains .....	13
2.1.3 Primers for PCR-based amplification methods .....	13
2.1.4 Cloning vectors .....	14
2.1.5 Plant lines .....	15
2.1.6 Media, buffers, solutions .....	15
2.2 Methods .....	18
2.2.1 Plant growth conditions and seed sterilization .....	18
2.2.2 Genomic DNA extraction from plant material .....	18
2.2.3 PCR reaction .....	19
2.2.4 Mutant screen .....	20
2.2.5 pFASTG02-FMT reporter construct .....	20
2.2.6 Sequencing .....	21
2.2.7 <i>Agrobacterium</i> -mediated transformation of <i>Arabidopsis thaliana</i> .....	21
2.2.8 Screening and identification of transgenic <i>Arabidopsis</i> seed.....	22
2.2.9 Phenotypic quantification and statistical analysis .....	22
2.2.10 Transmission electron microscopy.....	23
2.2.11 Quantification and analysis of <i>Arabidopsis</i> root cells from transmission electron microscopy .....	23
<b>3. Results</b> .....	<b>26</b>
3.1 Identification of the <i>FMT</i> and <i>FIS1A</i> genes .....	26
3.1.1 Expression levels of <i>FMT</i> and <i>FIS1A</i> in response to salt stress.....	27

3.2 Overexpression of the <i>FMT</i> gene in <i>Arabidopsis thaliana</i> .....	28
3.3 Phenotypic analyses of the <i>fis1A</i> , <i>fmt</i> , and <i>FMT-OE</i> mutants.....	29
3.3.1 <i>fis1A</i> mutants have shorter roots and slightly shorter leaves .....	29
3.3.2 <i>fmt</i> mutants have shorter roots and leaves and take longer to flower .....	30
3.3.3 <i>FMT-OE</i> mutants have a lower rate of germination, take longer to germinate, and have shorter roots and leaves.....	31
3.4 Effects of salt stress on <i>fis1A</i> , <i>fmt</i> , and <i>FMT-OE</i> mutants and WT plants.....	34
3.5 Electron microscopy analysis of WT, <i>fis1A</i> , <i>fmt</i> , and <i>FMT-OE</i> plants.....	48
3.5.1 Salt stress affects various mitochondrial parameters in WT, <i>fis1A</i> , and <i>fmt</i> ...	51
3.5.2 Clustering is regulated by FMT and is sensitive to salt stress .....	57
<b>4. Discussion .....</b>	<b>60</b>
4.1 FMT regulates multiple cellular processes in a variety of organisms.....	60
4.2 <i>fmt</i> and <i>FMT-OE</i> mutants show deficits in root and leaf length, and delays in flowering and germination .....	63
4.2.1 Putative role of FMT in germination and flowering control in <i>Arabidopsis</i> ...	64
4.3 Changes in FMT expression affect mitochondrial size, number, and clustering in columella cells.....	65
4.4 <i>fis1A</i> mutants have shorter roots and may regulate mitochondrial clustering.....	66
4.5 Salt stress affects various phenotypic and mitochondrial parameters.....	68
4.6 Conclusion and future perspectives.....	70
<b>References .....</b>	<b>72</b>
<b>Danksagung.....</b>	<b>82</b>
<b>Erklärung.....</b>	<b>83</b>
<b>Lebenslauf.....</b>	<b>84</b>

## Abbreviations

°C	degree Celsius
%	percent
cDNA	complementary DNA
Col-0	Columbia-0
DNA	deoxyribonucleic acid
dNTP	deoxynucleoside triphosphate
E. coli	<i>Escherichia coli</i>
e.g.	<i>exempli gratia</i> (Latin) for example
et al.	<i>et alterni</i> (Latin) and others
EtOH	ethanol
Fig.	figure
hr	hour
g	gram
GFP	green fluorescent protein
kb	kilo base pair
L	liter
M	Molar
min	minute
ml	mililiter
n	number
P value	Probability value
PCR	polymerase chain reaction
rpm	revolutions per minute
Sec	second
T-DNA	transfer DNA
WT	wild type
μl	microliter

## Nomenclature

The wild type genotype is written in italicized capital letters (e.g. *FMT*).

The mutant genotype is written in italicized lower case letters (e.g. *fmt*).

The polypeptide products of genes are written in non-italicized, capital letters (e.g. FMT).

## List of figures

Figure 1.	Mechanistic action of tropic growth in the <i>Arabidopsis thaliana</i> root.....	8
Figure 2.	Salt-regulated spatio-temporal expression in the <i>Arabidopsis</i> root.....	28
Figure 3.	Seeds of <i>Arabidopsis</i> plants transformed with pFASTG02-FMT give green fluorescence.....	29
Figure 4.	Phenotypic differences between WT, <i>fis1A</i> , <i>fmt</i> , and <i>FMT-OE</i> lines under control conditions.....	32
Figure 5.	Visualization of phenotypic differences between WT, <i>fis1A</i> , <i>fmt</i> , and <i>FMT-OE</i> lines under control conditions.....	33
Figure 6.	Salt stress affects days to germination and flowering, as well as leaf and root length in wild type <i>Arabidopsis</i> .....	35
Figure 7.	Salt stress affects days to germination and flowering, as well as leaf and root length in <i>fis1A</i> mutants.....	37
Figure 8.	Days to flowering is increased in <i>fis1A</i> mutants compared to the WT under salt-stressed conditions.....	39
Figure 9.	Salt stress affects days to germination in <i>fmt</i> mutants.....	41
Figure 10.	Days to flowering is increased and root and leaf length are decreased in <i>fmt</i> mutants compared to the WT under salt-stressed conditions.....	43
Figure 11.	Salt stress affects percent germination, days to germination, and leaf and root length in <i>FMT-OE</i> mutants.....	45
Figure 12.	Germination percentage and root length are decreased in <i>FMT-OE</i> mutants compared to the WT under salt-stressed conditions.....	47
Figure 13.	Differences in mitochondria between WT, <i>fis1A</i> , <i>fmt</i> , and <i>FMT-OE</i> lines under control conditions.....	50
Figure 14.	Comparison of various mitochondrial parameters between WT, <i>fis1A</i> , <i>fmt</i> , and <i>FMT-OE</i> lines.....	51
Figure 15.	Differences in mitochondria between WT, <i>fis1A</i> , and <i>fmt</i> lines under salt stress.....	53
Figure 16.	Visualization of the effects of salt stress on WT, <i>fis1A</i> , and <i>fmt</i> lines.....	54
Figure 17.	Comparison of various mitochondrial parameters between WT plants under control and salt-stressed conditions.....	55
Figure 18.	Comparison of various mitochondrial parameters between <i>fis1A</i> mutants under control and salt-stressed conditions.....	56
Figure 19.	Comparison of various mitochondrial parameters between <i>fmt</i> mutants under control and salt-stressed conditions.....	57
Figure 20.	Clustering patterns in WT, <i>fis1A</i> , <i>fmt</i> , and <i>FMT-OE</i> lines under control and salt-stressed conditions.....	59

## Abstract

Salt stress is known to have severe effects on plant health and fecundity, and mitochondria are known to be an essential part of the plant salt stress response. *Arabidopsis thaliana* serves as an excellent model to study the effects of salt stress as well as mitochondrial morphology. *Arabidopsis* contains several homologues to known mitochondrial proteins, including the fission protein FIS1A, and FMT, a homologue of the CLU subfamily. We sought to examine the effects of salt stress on knockout lines of FIS1A and FMT, as well as a transgenic line overexpressing FMT (*FMT-OE*) in columella cells in the root cap of *Arabidopsis*. *fmt* mutants displayed defects in both root and leaf growth, as well as a delay in flowering time. These mutants also showed a pronounced increase in mitochondrial clustering and number. *FMT-OE* mutants displayed severe defects in germination, including a decrease in total germination, and an increase in the number of days to germination. *fis1A* mutants exhibited shorter roots and slightly shorter leaves, as well as a tendency towards random mitochondrial clustering in root cells. Salt stress was shown to affect various mitochondrial parameters, including an increase in mitochondrial number and clustering, as well as a decrease in mitochondrial area. These results reveal a previously unknown role for FMT in germination and flowering in *Arabidopsis*, as well as insight into the effects of salt stress on mitochondrial morphology. FMT, along with FIS1A, may also help to regulate mitochondrial number and clustering, as well as root and leaf growth, under both control and salt-stressed conditions. This has implications for both FMT and FIS1A in whole-plant morphology as well as the plant salt stress response.

## **Zusammenfassung**

Salzstress hat schwerwiegende Auswirkungen für die Gesundheit und Fruchtbarkeit von Pflanzen, und Mitochondrien sind ein wesentlicher Teil der Salzstressantwort. Die *Arabidopsis thaliana* dient als ein hervorragendes Modell, um die Auswirkungen von Salzstress sowie mitochondriale Morphologie zu studieren. *Arabidopsis* enthält mehrere Homologe zu bekannten mitochondrialen Proteinen, einschließlich des Spaltungsproteins FIS1A, und FMT, ein Homolog des CLU Unterfamilie. Das Ziel war es, die Auswirkungen von Salzstress auf die Knockout-Linien FIS1A und FMT sowie eine transgene Linie überexprimierenden FMT (*FMT-OE*) in Columella-Zellen in der Wurzelkappe von *Arabidopsis* zu untersuchen. *Fmt*-Mutanten zeigten Defekte im Wurzel- und Blattwachstum, sowie eine Verzögerung in der Blütezeit. Diese Mutanten zeigten auch eine deutliche Zunahme der mitochondrialen Cluster-Bildung und Anzahl. *FMT-OE*-Mutanten zeigten schwere Defekte in der Keimung, einschließlich einer Verringerung der Gesamtkeime und eine Zunahme in der Anzahl der Tage zur Keimung. *fis1A*-Mutanten zeigten kürzere Wurzeln und etwas kürzere Blätter, sowie eine Tendenz zur zufälligen mitochondrialen Clustering in Wurzelzellen. Salzstress hatte Einfluss auf verschiedene mitochondriale Parameter, einschließlich einer Zunahme der Mitochondrienzahl und -gruppierung, sowie eine Abnahme des mitochondrialen Bereichs. Diese Ergebnisse zeigen eine bisher unbekannte Rolle für FMT in Keimung und Blüte in *Arabidopsis*, sowie einen Einblick in die Auswirkungen von Salzstress auf die mitochondriale Morphologie. FMT, zusammen mit FIS1A, kann auch helfen, mitochondriale Anzahl und Cluster-Bildung sowie Wurzel- und Blattwachstum zu

regulieren, sowohl unter Kontroll- und Salzstressbedingungen. Dies hat Auswirkungen auf beide FMT und FIS1A in Ganzpflanzenmorphologie und für die Salzstressantwort.

# **1. Introduction**

The driving force behind agriculture is an ever-increasing demand to grow food to sustain a rapidly increasing global population. The pressure to continually produce more crops in a wider variety of environments further drives the need for scientists to design and develop more stress-resistant crop plants. Crops that can endure the effects of exposure to multiple abiotic or biotic stresses while maintaining fecundity will prove to be the most useful for farmers operating in the growing global agricultural market.

## **1.1 Effects of soil salinity on agriculture**

The effects of stress on the proper development and growth of crops currently poses a severe threat to agriculture. One of the most damaging stresses is salinity, or increased levels of salt in the soil. All soil contains some level of salt, and many salts, such as nitrates, are essential plant nutrients. However, the increased use of irrigation and brackish water, as well as increased runoff and poor drainage, has led to high levels of excess salt in the soil. Additional sources of excess salt include inorganic fertilizers, manure, compost, mineral weathering, seawater intrusion into aquifers, and ice melters used on sidewalks and roads (Hasegawa et al., 2000, Carillo et al., 2011). In addition to sodium ( $\text{Na}^+$ ), irrigation waters may also contain higher levels calcium ( $\text{Ca}^{2+}$ ) and magnesium ( $\text{Mg}^{2+}$ ). However, when the water evaporates, the  $\text{Ca}^{2+}$  and  $\text{Mg}^{2+}$  precipitate into carbonates, leaving behind high levels of  $\text{Na}^+$ . Soil is considered saline when solution extracted from the soil has an electrical conductivity of  $4\text{dS m}^{-1}$  (decisiemens per meter), where  $4\text{dS m}^{-1} \approx 40\text{mM NaCl}$  or more. In irrigated land, salt levels can vary both

spatially and seasonally, and additional factors such as temperature, pressure, and humidity, can also affect salt levels (Cardon, 2007). It has been estimated that more than 45 million hectares of crops had been damaged by salinization, and 1.5 million hectares were deemed unusable each year (Munns & Tester, 2008). This is predicted to result in up to a 50% reduction in arable land by the year 2050 (Pitman & Läuchli, 2002).

## **1.2 Effects of soil salinity on plants**

Plants can be divided into two major categories for coping with salt tolerance. Glycophytes (salt-intolerant plants) evolved under conditions of low soil salinity and cannot grow or are severely inhibited at salt concentrations above 150mM NaCl. Most glycophytes can tolerate salt concentrations of ~50mM NaCl and below, although some can survive at higher concentrations. Halophytes (salt-tolerant plants) evolved in places with highly salinized soil, and can survive salinity in excess of 300-400mM (Hasegawa et al., 2000).

High salinity affects plants in two main ways: osmotic stress reduces the ability of the plant to extract water from the soil, and high concentrations of salts within the plant can cause damage to plant structures and impede many physiological and biochemical processes. Initial exposure to salt stress has an immediate effect on the plant, rapidly increasing the levels of osmotic and ionic stress. Osmotic stress occurs as a result of excess  $\text{Na}^+$  ions in the surrounding soil compared to internal concentrations in the root, which generates an external osmotic pressure that reduces water influx into the root. The result is a water deficit similar to those seen under drought conditions. This can lead to impaired growth and decreased viability, as water and key nutrients are unable to be

transported throughout the plant. Osmotic stress is believed to occur for the duration of salt exposure, resulting in increased stomatal closure and an inhibition of cell division and expansion. Long-term exposure to salt stress can also trigger ionic stress, which occurs as a result of increased  $\text{Na}^+$  accumulation in the leaves, which can disrupt protein synthesis and enzymatic activity, often triggering premature senescence in older leaves. This reduces the photosynthetic availability of the plant, further impairing plant growth (Hasegawa et al., 2000, Carillo et al., 2011). However, despite the damaging effects of salinity, plants have evolved a variety of mechanisms to counter-act salt stress over both the short- and long-term.

### **1.3 Plant responses to salinity**

Plants display a wide variety of responses to salinity, and as a result exhibit several whole-organism phenotypic changes. Some of these changes are side effects, while some occur as a direct response to salt stress. One example of a side-effect-derived change occurs when excess  $\text{Na}^+$  ions are actively shuttled out of the plant shoot and into the leaves, in order to allow for  $\text{K}^+$  accumulation in the shoot to help balance the  $\text{K}^+/\text{Na}^+$  ion ratio. However, when  $\text{Na}^+$  ions reach a critical level in the leaves they begin to stunt growth, eventually leading to leaf necrosis and eventual plant death (Hauser & Horie, 2010). Direct changes in response to salt stress include the reorganization of root system architecture (RSA), which allows for a rapid response to changes in  $\text{NaCl}$  in the soil (Malekpoor Mansoorkhani et al., 2014, Jones & Ljung, 2012). Other direct responses include a suppression of germination or a delay in flowering, most likely as a way of waiting until conditions are more ideal to grow or produce offspring seeds (Srivastava et

al., 2016, Conti et al., 2008). The genes and pathways that control these phenotypic changes are known in some cases, but the overall etiology underlying the various salt stress responses remain elusive. In addition, the roles of various organelles, including mitochondria, which are known to play a role in the stress response, remain poorly understood. Below is a discussion of some of the most well understood plant responses to stress, including salinity, and the role of mitochondria in each of these responses.

#### **1.4 Mitochondrial response to stress**

Mitochondria are known to play key roles in a variety of plant responses to salt stress.

These responses usually involve highly conserved mechanisms, and include the hypersensitive response (HR) and programmed cell death (PCD), the SOS Pathway, the reorganization of Root System Architecture and salt-avoidance tropism.

##### **1.4.1 The hypersensitive response and programmed cell death**

A common response to stress is the plant hypersensitive response (HR). In response to pathogenic attack, cells will undergo programmed cell death (PCD) in the surrounding area under attack, disabling a virus from co-opting host machinery from neighbouring cells, eventually rendering the virus unable to reproduce, and thus eventually die. PCD is also a well-characterized mechanism in animals, and many of the basic regulatory mechanisms that underlie this response are similar in both plants and animals. Indeed, short-term salinity stress was shown to induce PCD in a manner similarly to animals (Andronis & Roubelakis-Angelakis, 2010). One shared feature between animal and plant PCD is the role of the mitochondria in the regulation of PCD. In both plants and animals,

mitochondria may initiate apoptosis in response to changes in various cellular regulators, such as cytosolic calcium and cellular pH, or indicators of cellular energy availability, such as ATP, ADP, NADH, and NADPH. Various other proteins may also be activated in response to stress and can associate with and modify the permeability of the outer mitochondrial membrane (OMM), including the opening of the mitochondrial permeability transition pore (mPTP). This leads to a decrease in the mitochondrial membrane potential and the release of various cell death activators from within the mitochondrion, including the apoptosis-inducing factor (AIF) and cytochrome *c* (Lam et al., 2001, Morel & Dangl, 1997, Heath, 2000).

#### **1.4.2 The SOS Pathway**

The SOS (Salt Overly Sensitive) pathway was originally identified in a genetic screen to find plants that were hypersensitive to salt stress (Wu et al., 1996, Zhu et al., 1998). The *sos1*, *sos2*, and *sos3* mutants were shown to have severely impaired growth on media with an excess of Na<sup>+</sup> or Li<sup>+</sup> ions, or a deficit of K<sup>+</sup> ions, but grew similarly to wild type plants under normal growth conditions. These mutants also grew normally under general osmotic or drought stress, which indicates that the *SOS* genes play a specific role in mediating the ionic response to salt stress in plants. The SOS pathway is activated when excess Na<sup>+</sup> is sensed by the cell, leading to an increase of cytoplasmic Ca<sup>2+</sup>. This Ca<sup>2+</sup> spike is sensed by *SOS3*, which activates *SOS2*, forming a SOS3-SOS2 kinase complex. This complex activates *SOS1*, an Na<sup>+</sup>/H<sup>+</sup> antiporter, which pumps excess Na<sup>+</sup> from the cytoplasm and into extracellular space or the root medium (Ji et al., 2013). Mitochondria are known to buffer cytosolic calcium following a spike in concentration (Vandecasteele

et al., 2001), however, the extent of their role in the SOS pathway has not been well studied.

### **1.4.3 Reorganization of Root System Architecture and salt-avoidance tropism**

The shape and structure of the roots, as well as their spatial configuration within the soil, determines the root system architecture (RSA) of a plant. The RSA of an individual plant is determined by the unique and heterogeneous distribution of edaphic resources (Malamy, 2005, de Dorlodot et al., 2007). In response salt stress, the RSA is altered such that primary root elongation is inhibited, while lateral root (LR) formation increases in response to lower concentrations of NaCl, but is inhibited at higher concentrations (Wang et al., 2008, Zolla et al., 2010). These responses are mediated by changes in cell length and number (Duan et al., 2015), and mitochondria are known to play a role in this regulation (van der Merwe et al., 2009).

In addition to changes in RSA, plant roots may change their direction of growth to avoid excess salt in the soil. Roots primarily grow downwards towards the gravity vector, a phenomenon known as positive gravitropism, or tropic growth. Although it is not known exactly how roots recognize the gravity vector, the “starch statolith hypothesis” posits that amyloplasts in the columella cells of the root cap sediment to the “bottom” of the cell, directing the orientation of growth (Fig. 1A,B) (Sato et al., 2015). When it is necessary to avoid NaCl ions in the soil, roots can exhibit negative gravitropism and grow against the gravity vector, a process known as salt-avoidance tropism, which helps minimize exposure to stress. How the root is able to sense excess salt and subsequently change its direction of growth is not well understood. Sun et al. (2008) found that, upon

exposure of the root to salt stress, two main responses were initiated: 1) rapid degradation of amyloplasts, followed by 2) root bending resulting in negative gravitropism. Amyloplast degradation may be regulated by the SOS pathway, and root bending is likely triggered by PIN2, an auxin efflux carrier, that asymmetrically distributes auxin in the root leading to root curvature (Ottenschlager et al., 2003). However, it is highly likely that other proteins, including those involved with mitochondria, act to regulate salt-avoidance tropism and root bending, as well as reorganization of RSA. Zhang et al. (2015) recently discovered a mitochondrial-localized protein, SSR1, which regulates root growth and architecture, and is required for PIN2 trafficking. This indicates a clear role for mitochondria and their associated proteins in the regulation of root system architecture, with implications for a role in the changes of this architecture in response to salt stress.

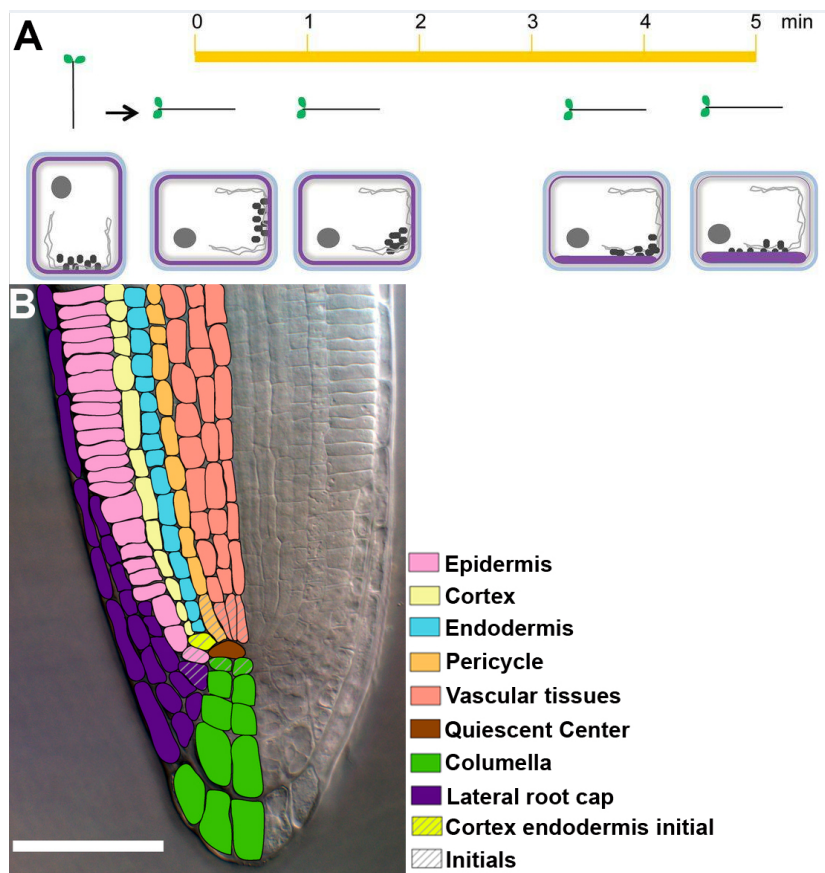


**Figure 1: Mechanistic action of tropic growth in the *Arabidopsis thaliana* root.** A) Following a 90° turn, statoliths in columella cells start to fall to the bottom of the cell, and are fully sedimented by 5 min. B) Diagram of an *Arabidopsis* root; columella cells are labelled in green (adapted from Barrada et al. (2015); Sato et al. (2015)). Scale bar = 50 µm.

### 1.5 Mitochondrial clustering in response to stress

A less well-understood response of mitochondria to stress is that of mitochondrial clustering. Mitochondrial trafficking and movement is known to be essential for proper mitochondrial and cellular function, but under stress conditions, mitochondria display altered motility and distribution, which can have deleterious consequences for an organism (Chen & Chan, 2009, Nunnari & Suomalainen, 2012). In plants, mitochondrial clustering and/or arrest of mitochondrial motility has been recognized as a response to various abiotic and biotic stresses, including in response to the application of reactive

oxygen species, heat shock (Scott & Logan, 2008), methyl jasmonate (Zhang & Xing, 2008), oxylipin, 9-hydroxy-10,12,15-octadecatrienoic acid (Vellosillo et al., 2013), and UV light exposure (Gao et al., 2008). However, the mechanisms that give rise to this mitochondrial clustering are not known. Knockouts of the highly conserved gene *CLU* (CLUstered mitochondria) was shown to induce mitochondrial clustering in a variety of eukaryotes, including *Dictyostelium*, *Saccharomyces cerevisiae*, *Drosophila*, and *Arabidopsis* (Zhu et al., 1997, Fields et al., 1998, Cox & Spradling, 2009, El Zawily et al., 2014). However, the role of mitochondrial clustering in plants in response to stress, including salt stress, has not previously been investigated.

### **1.6 The FMT/CLU and FIS1A genes in eukaryotes**

The first member of the *CLU* family to be identified was *cluA* in *Dictyostelium*, and this gene was found to be necessary for the correct dispersion of mitochondria within the cell (Zhu et al., 1997). Fields et al. (1998) demonstrated that *CLUI*, a functional homologue of *cluA* in *Saccharomyces cerevisiae* (*S. cerevisiae*), performed a similar function. *clu1Δ* cells, which had their *CLUI* genes deleted, formed loose clusters of mitochondria within the cytoplasm. Cox and Spradling (2009) characterized the *CLU* gene in *Drosophila*, known as *clueless*, and found that *clueless* mutants exhibited mitochondrial clustering within cells. Flies that were homozygous for the *clu* defect (*clu*<sup>d08713</sup> or *clu*<sup>f04554</sup>) lived for only 3-7 days, were smaller than WT flies, sterile, and could not fly.

The *CLU* homologue in *Arabidopsis*, *FMT* (friendly mitochondria), was originally identified by Logan et al. (2003) in a mutant screen to find candidate genes involved in mitochondrial dynamics and morphology in higher plants. *FMT* is 26% identical and

41% similar to the *Dictyostelium* cluA protein and, like cluA, also contains a TPR (tetratricopeptide repeat)-like domain. FMT is 20% identical and 34% similar to the *S. cerevisiae* Clu1p protein. All CLU homologues that have been studied possess a TPR domain, and it remains the most highly conserved portion of the *CLU* gene throughout its evolution between species. Tetratricopeptide repeats are found in genes in all species, and are known for their ability to mediate protein interactions between partner proteins. In plants, they are found in a variety of genes involved in stress and hormone signalling. One example is *TTL1* (Tetratricopeptide-repeat thioredoxin-like 1), which is known to be a positive regulator of the ABA- (abscisic acid) mediated stress response. Knockouts of *TTL1* increased salt and osmotic sensitivity during seed germination and in later development (Rosado et al., 2006). *Drosophila* clueless was also found to bind nuclear-encoded mitochondrial mRNAs through its TPR domain and direct them to the mitochondrial outer membrane where they could potentially be positioned for co-translational import into mitochondria (Sen et al., 2015).

Electron microscopy analysis of leaf tissue of *fmt* mutant plants initially revealed the similar phenotype of mitochondrial clustering that was observed in other species (Logan et al., 2003). Further analysis by El Zawily et al. (2014) revealed that FMT might play a role in intermitochondrial association and quality control. It was hypothesized that FMT may function as a fusion protein, as there are currently no known homologues to conserved fusion proteins in plants. However, plant fission proteins are highly conserved in plants, including DRP and FIS1A. Mitochondrial fission proteins also play an important role in the stress response by facilitating the division of a partially damaged

mitochondrion into one healthy and one damaged mitochondrion that can be targeted for degradation (Youle & van der Bliek, 2012).

The mitochondrial division machinery used by *Arabidopsis* is conserved across animals, plants, and fungi (for review see Praefcke & McMahon, 2004). In plants, dynamin-like proteins (DLPs) have been shown to be necessary for the division of mitochondria (Aung & Hu, 2012). DRP3A and DRP3B (previously known as ADL2a and ADL2b, respectively) in *Arabidopsis* are homologous to the Dnm1 and Drp1/DLP1 proteins found in yeast and mammals, respectively. These proteins are part of a DRP subclade that is well conserved across eukaryotic species and contain the GTPase, MD, and GED domains (Miyagishima et al., 2008). DRP3A and DRP3B both localize to mitochondria and were shown to play a dual role in the final scission of both organelles (Aung & Hu, 2012). *Arabidopsis* also contains two proteins homologous to FIS1 in *S. cerevisiae* and humans: FIS1A (also known as BIGYIN1), and FIS1B (also known as BIGYIN2) (Mozdy et al., 2000, Tieu & Nunnari, 2000, Smirnova et al., 2001, James et al., 2003, Youle & Karbowski, 2005). Similar to their yeast and mammalian counterparts, these plant proteins localize to the outer mitochondrial membrane (OMM) and play a key role in mitochondrial division (Logan, 2010). *Arabidopsis fis1A* mutants had a reduction in the number of mitochondria per cell, with simultaneous increases in the size of individual mitochondrion in protoplasts and leaves (Scott et al., 2006). This provides further evidence for the role of FIS1A in mitochondrial fission in plants. However, the role of fission and FIS1A during salt stress is not currently known.

## 1.7 Thesis aims

The plant salt stress response remains an important mechanism for maintaining growth and survival under ever-changing environmental conditions, and mitochondria are known to be essential for the mediation of this response. However, how this organelle exerts its control, and what proteins are involved, is not well understood. Two mitochondrial proteins, FIS1A, and FMT, are known to be essential for mitochondrial quality control. Given the role of mitochondria in the salt stress response, and given the fact that salt stress is sensed first in the soil by the roots, we wanted to examine the effects of a knockout of either *FMT* or *FIS1A*, as well as an overexpression of *FMT*, in mitochondria in columella cells of the roots under both control and salt-stressed conditions. We also wanted to examine the phenotypic effects of these mutants under both control and salt-stressed conditions. Additionally, since the effects of salt stress on mitochondrial morphology in wild type plants had not previously been characterized, we wanted to examine various mitochondrial parameters in the columella cells of the roots of wild type plants exposed to salt stress. The aim is to further our understanding of the role of mitochondria in salt stress and as such add to the canon of knowledge of the salt stress response as a whole.

## 2. Material and Methods

### 2.1 Material

#### 2.1.1. Antibiotics

**Table 1:** Antibiotics used in this study

Antibiotic	Solvent	Stock concentration (mg/ml)	Working concentration (µg/ml)
Gentamicin	H <sub>2</sub> O	10	50
Kanamycin	H <sub>2</sub> O	50	50
Spectinomycin	H <sub>2</sub> O	100	75

#### 2.1.2 Bacterial strains

##### *E. coli*

One Shot TOP10 (Invitrogen, USA)

DH5α (Invitrogen, USA)

##### *Agrobacterium tumefaciens*

GV3101 (pMP90)

#### 2.1.3 Primers for PCR-based amplification methods

All primers were purchased from the W.M. Keck Foundation (Yale School of Medicine, New Haven, CT). Primer sequences are listed in Table 2.

**Table 2:** Primers used in this study

<b>Primer Name</b>	<b>Sequence (5' → 3')</b>	<b>Notes</b>
<b>T-DNA Primers</b>		
LBb1.3	ATTTTGCCGATTTTCGGAAC	Left border primer for T-DNA insertion
FIS1A LP	AAGATCCTCCTTGACCTCGAC	Left primer for FIS1A (SALK_006512C)
FIS1A RP	GCTGATTGGAGACAAGCTTTG	Right primer for FIS1A (SALK_006512C)
FMT LP	ATACCTGCAGCAGTTTGCAAC	Left primer for FMT (SALK_046271C)
FMT RP	CTAGCGCCAACAGCTCTACTG	Right primer for FMT (SALK_046271C)
<b>Gateway Primers</b>		
attB1 FP FMT	GGGGACAAGTTTGTACAAAAAAGCAG GCTTCATGGCTGGGAAGTCGAAC	attB1 Forward primer for FMT
attB1 RP FMT	GGGGACCACTTTGTACAAGAAAGCTG GGTCTTTTTTGGCTTTTGTCTTCTT	attB1 Reverse primer for FMT
<b>Sequencing Primers</b>		
M13 FP	GTAAAACGACGGCCAG	Forward sequencing primer for pDONR 221
M13 RP	CAGGAAACAGCTATGAC	Reverse sequencing primer for pDONR 221
FMT Seq1	ATGGCTGGGAAGTCGAAC	FMT Sequencing Primer 1
FMT Seq2	ATCTATCAGAGCGCATGTTCA	FMT Sequencing Primer 2
FMT Seq3	GAGCAGAAGAAGCACTTACCA	FMT Sequencing Primer 3
FMT Seq4	GCCATAGGGTTGTTGCTCAG	FMT Sequencing Primer 4
FMT Seq5	AAGAGGAGATAGCTGCTGATG	FMT Sequencing Primer 5
FMT Seq6	TAATCTTTGCCAAAAGGTTGGTG	FMT Sequencing Primer 6
FMT Seq7	AAAATGAGAGACTTCTTGGTCCT	FMT Sequencing Primer 7
FMT Seq8	AACAGAAAACCTGGCTCCTG	FMT Sequencing Primer 8

#### 2.1.4 Cloning vectors

The pDONR 207 (Invitrogen) and pFASTG02 (p\*7FWG2, Plant Systems Biology) vectors were used for cloning in this study.

### **2.1.5 Plant lines**

All experiments were performed using *Arabidopsis thaliana* Col-0 wild type plants or mutants in the Col-0 background. *fmt* homozygous mutants (SALK\_046271C), and *fis1A* homozygous mutants (SALK\_006512C) were obtained from ABRC (Arabidopsis Biological Resource Center, Ohio State University, Columbia, OH, USA). All homozygous mutant lines were confirmed by PCR.

### **2.1.6 Media, buffers, solutions**

#### **Media**

##### LB Media

25g LB Broth

ddH<sub>2</sub>O to 1L

For solid medium, 2% Agar was added to the above medium.

After autoclaving at 121°C for 20 mins and cooling to 55°C, antibiotics were added.

##### MS-Agar Media (pH 5.7)

4.3g MS Salts

0.5g MES

10g Agarose

ddH<sub>2</sub>O to 1L

After autoclaving at 121°C for 20 mins and cooling to 55°C, media was poured into plates.

#### 125mM NaCl Stress Media

800 ml MS-Agar Media

7.3g NaCl

ddH<sub>2</sub>O to 1L

After autoclaving at 121°C for 20 mins and cooling to 55°C, media was poured into plates.

#### **Buffers**

##### CTAB Buffer (100mL, pH 5.0)

2 g CTAB (Hexadecyltrimethylammonium bromide)

10 ml 1 M Tris pH 8.0

4 ml 0.5 M EDTA pH 8.0

28 ml 5 M NaCl

40 ml ddH<sub>2</sub>O

##### Phosphate Buffer Stock A

27.6g NaH<sub>2</sub>PO<sub>4</sub>·H<sub>2</sub>O

ddH<sub>2</sub>O to 1L

### Phosphate Buffer Stock B

28.4g/L Na<sub>2</sub>HPO<sub>4</sub>·H<sub>2</sub>O

ddH<sub>2</sub>O to 1L

### 0.2M Phosphate Buffer (pH 6.8)

51% Phosphate Buffer Stock A

49% Phosphate Buffer Stock B

## **Solutions**

### Fixative

0.5% (wt/vol) formaldehyde

3% (wt/vol) gluteraldehyde

0.1M Phosphate Buffer (pH 6.8)

### 1% osmium tetroxide fixative

1ml OsO<sub>4</sub> (4%)

3ml 0.1M Phosphate Buffer (pH 6.8)

### 2% uranyl acetate staining solution

0.4g uranyl acetate

20ml H<sub>2</sub>O

## **2.2 Methods**

### **2.2.1 Plant growth conditions and seed sterilization**

Arabidopsis seeds were sown directly on Fafard #2 soil mixture (Sun Gro Horticulture) and were grown under 16-hr light/8-hr dark (long-day) photoperiods at 22°C +/-1°C under cool-white light at 100  $\mu\text{mol m}^{-2} \text{s}^{-1}$ . For experiments done on sterilized MS (Murashige Skoog)-Agar media, seeds were first surface sterilized by washing in 70% (v/v) ethanol for 5 sec, and this wash was replaced by 0.1% triton X-100 in 50% bleach (v/v) for 5 sec before five rinses in autoclaved ddH<sub>2</sub>O. Seeds were then plated on 100 x 100 x 15 mm square petri dishes (Ted Pella), and plates were stratified at 4°C for three days in the dark to synchronize germination. Plates were then moved to long-day photoperiod conditions at 22°C +/-1°C under cool-white light at 100  $\mu\text{mol m}^{-2} \text{s}^{-1}$ . Plates were placed at an angle to allow for root growth along the surface of the agar. For salt-stressed growth conditions on plates, seeds were plated on MS-Agar plates supplemented with 125mM NaCl. For salt-stressed conditions in the soil, the following NaCl concentrations were added when the plants were watered, beginning one week after germination and increasing every week: 50mM NaCl, 75mM NaCl, 100mM NaCl, 125mM NaCl, 140mM NaCl.

### **2.2.2 Genomic DNA extraction from plant material**

Genomic plant DNA was extracted using the CTAB method. 200 mg plant leaf tissue was ground in eppendorf tubes and 500 $\mu\text{l}$  CTAB Buffer was added. The mixture was incubated for 15 minutes at 55°C and tubes were then centrifuged at 13,000 rpm for 5

minutes. The supernatant was transferred to a new eppendorf tube and 250 µl of 24:1 chloroform:isopropanol was added and mixed by inversion. The tubes were spun at 13,000 rpm for 1 minute. The upper aqueous phase was transferred to a new eppendorf tube and 50 µl of 7.5M ammonium acetate and 500 µl of ice-cold absolute ethanol were added. The tubes were mixed slowly by inversion and placed at -20°C for 1 hour to precipitate the DNA. Tubes were then spun at 13,000 rpm for 1 minute to form a pellet. The supernatant was removed and the pellets were dried for 15 minutes at room temperature. The pellet was resuspended in 50 µl DNase-free H<sub>2</sub>O and stored at 4°C.

### 2.2.3 PCR reaction

All PCR reactions were done using a Bio Rad C1000 Touch Thermal Cycler. For genotyping, a standard PCR reaction mix was used, using PCR Supermix (Invitrogen). The standard PCR reaction mix (Table 3) and standard PCR thermal profile (Table 4) are shown below.

**Table 3:** Standard PCR reaction mix

<b>Reagent</b>	<b>Amount</b>	<b>Concentration</b>
PCR Supermix	20 µl	1.1X
Forward Primer	0.5 µl	10 µM
Reverse Primer	0.5 µl	10 µM
DNA Template	1 µl	100-150 ng
H <sub>2</sub> O	3 µl	N/A
	<b>25 µl</b>	

**Table 4:** Standard PCR thermal profile

Step	Temperature	Time	Cycles
Initial denaturation	95°C	3 min.	
Denaturation	95°C	30 sec.	20-35
Annealing	55°C	30 sec.	20-35
Extension	72°C	20-300 sec.	20-35
Final extension	72°C	3 min.	
Hold	4°C	∞	

#### 2.2.4 Mutant screen

Both FMT and FIS1A were screened for available T-DNA insertion lines on TAIR (The Arabidopsis Information Resource, <http://www.arabidopsis.org/>). PCR was used to test whether the T-DNA was inserted at the predicted insertion site. All T-DNA insertions were confirmed via PCR using left and right primers flanking the genomic sequence, and a border primer located within the T-DNA sequence (see Table 2 for primer list).

#### 2.2.5 pFASTG02-FMT reporter construct

pFASTG02-FMT was constructed by subcloning a FMT cDNA fragment of the expected size into the pDONR 221 vector (Gateway, Invitrogen). In order to PCR amplify the cDNA fragment, the following primers were used: forward (attB1 FP FMT),

5'-GGGGACAAGTTTGTACAAAAAAGCAGGCTTCATGGCTGGGAAGTCGAAC-

3', and reverse (attB1 RP FMT),

5'-GGGACCACTTTGTACAAGAAAGCTGGGTCTTTTTTGGCTTTTTGCTTCTT-3'.

The fragment was subsequently cloned into pFASTG02 (Shimada et al., 2010) according to the manufacturer's protocol (Invitrogen). This vector construct, pFASTG02-FMT, allowed for overexpression of the *FMT* gene under the control of the cauliflower mosaic

virus (CaMV) 35S promoter. The construct was sequenced to identify an error-free clone and subsequently transformed into wild type Col-0 plants by means of *Agrobacterium*-mediated transformation using the *Agrobacterium tumefaciens* strain GV3101 (pMP90).

### **2.2.6 Sequencing**

All sequencing reactions were done by the W.M. Keck Foundation (Yale School of Medicine, New Haven, CT).

### **2.2.7 *Agrobacterium*-mediated transformation of *Arabidopsis thaliana***

The pFASTG02-FMT vector was transformed into the *Agrobacterium tumefaciens* strain GV3101 via electroporation and colonies were selected on LB media plates supplemented with 50 µg/ml spectinomycin. Single colonies were picked and cultured in LB media supplemented with 50 µg/ml spectinomycin and grown to  $OD_{600} = 0.6$ . The cultures were then centrifuged at 13,000 rpm for 30 minutes and the pellets were resuspended in a 5% sucrose solution. Plants were dipped according to Clough and Bent (1998) with the following modifications: Silwet L-77 was added to the sucrose solution to a concentration of 0.05% and *Arabidopsis* plants with emerging flower stems were dipped in the solution for five seconds. The plants were then kept under long-day photoperiod conditions under transparent covers at 22°C +/- 1°C under cool-white light at 100 µmol m<sup>-2</sup> s<sup>-1</sup> for three days. Covers were removed and plants were grown until seed was mature. Mature seeds were collected and screened to identify transgenic seed expressing the pFASTG02-FMT vector.

### **2.2.8 Screening and identification of transgenic *Arabidopsis* seed**

Seeds from transformed plants were collected and screened for transgenic individuals containing the pFASTG02-FMT vector by the expression of green fluorescence in the seed coat by fluorescence microscopy under 4X magnification with the Zeiss Axioplan 2 fluorescence microscope (Carl-Zeiss, Germany). Transgenic seeds were then sown to produce T<sub>2</sub> seeds. Lines with a single transgene insertion were identified by an ~3:1 segregation ratio of GFP to no-GFP, respectively. Seeds from this line were sown to identify a homozygous plant (FMT-3), which was identified by T<sub>3</sub> seed that exhibited 100% GFP fluorescence. Seeds from line FMT-3 were collected and used in subsequent experiments.

### **2.2.9 Phenotypic quantification and statistical analysis**

*Arabidopsis* plants were grown to three weeks old in the soil under control or salt-stressed conditions described above. For leaf length quantification, three leaves were selected and measured from the base of each leaf to the tip using a ruler. For quantification of root length under control conditions, *Arabidopsis* plants were grown on control MS-Agar plates and roots were measured using a ruler at days seven and fourteen. For quantification of root length under salt-stressed conditions, *Arabidopsis* plants were grown on control MS-Agar plates for one week, and then transplanted to either control or 125mM NaCl MS-Agar plates for one week and roots were measured at day fourteen. For MS-Agar plate experiments, at least 20 replicates were used for each experiment, and each experiment was repeated three times. For soil experiments, at least 10 replicates were used for each experiment, and each experiment was repeated three times. Mutant

genotypes were compared to the wild type under both control and salt-stressed conditions. Statistical differences were determined using Student's two tailed *t* test, one-way analysis of variance (ANOVA), or two-way ANOVA, where appropriate.

#### **2.2.10 Transmission electron microscopy**

*Arabidopsis* seedlings were grown on MS-Agar plates for one week, and were then transferred to either 125mM NaCl MS-Agar plates or MS-Agar plates without the addition of NaCl for an additional week. Fixation and embedding of 14-day-old root samples was done according to Wu et al. (2012) with the following modifications: Durcupan epoxy resin (Sigma) was used for infiltration, tissue was collected on single slot copper grids (EMS) coated with formvar, and no post-sectioning heavy metal staining was used. Transverse sections were cut ~30  $\mu$ M deep into the columella of the root and subsequently viewed under a Tecnai 12 Transmission Electron Microscope (FEI, USA). At least ten cells from four biological samples each of WT, *fis1A*, *fmt*, and *FMT-OE* roots were examined for control experiments, and at least ten cells from two biological samples each of WT, *fis1A*, or *fmt* roots were examined for salt-stressed experiments. Due to the difficulty in preserving salt-stressed *FMT-OE* mutants during the fixation and embedding process, these mutants were not observed for TEM.

#### **2.2.11 Quantification and analysis of *Arabidopsis* root cells from transmission electron microscopy**

Using Fiji, an individual cell, nucleus, vacuole, and mitochondria were traced and measured to give the following parameters: area, aspect ratio (AR), number of

mitochondria per cell, and centroid XY coordinates of each individual mitochondrion. Mitochondrial coverage was calculated as a percent using the following formula:  $((\text{Cytoplasmic area} - \text{mitochondrial area}) * 100)$ , where cytoplasmic area = (Cell area - nuclear area - vacuole area), and mitochondrial area is the sum of all the areas of the individual mitochondria within the cell.

Mitochondrial clustering was calculated using the Nearest Neighbor Distances (NND) tool in the BioVoxel toolbox plugin in Fiji ([http://imagej.net/BioVoxel\\_Toolbox](http://imagej.net/BioVoxel_Toolbox)). The NND tool measures the average nearest neighbor ratio (ANN), which is calculated as the distance from the center of a particular particle (in this case a mitochondrion) to the center of its nearest neighbor. The average of all the nearest neighbor distances are then taken. If the average distance is less than the average of a hypothetical random distribution, the mitochondria are considered clustered. If the average distance is greater than a hypothetical random distribution, the mitochondria are considered dispersed. The average nearest neighbor ratio (ANN) is given as:

$$ANN = \frac{\bar{D}_O}{\bar{D}_E}$$

where  $\bar{D}_O$  is the observed mean distance between each feature and its nearest neighbour:

$$\bar{D}_O = \frac{\sum_{i=1}^n d_i}{n}$$

and  $\bar{D}_E$  is the expected mean distance for the features given in a random pattern:

$$\bar{D}_E = \frac{0.5}{\sqrt{n/A}}$$

In the above equations,  $d_i$  equals the distance between feature  $i$  and its nearest neighboring feature,  $n$  corresponds to the total number of features, and  $A$  is the area of a minimum enclosing rectangle around all features.

The average nearest neighbor z-score for the statistic is calculated as:

$$Z = \frac{\bar{D}_O - \bar{D}_E}{SE}$$

where:

$$SE = \frac{0.26136}{\sqrt{n/A}}$$

If the ANN is less than 1, then the pattern exhibits clustering. If the ANN is greater than 1, the pattern trends towards dispersion. If the ANN is exactly 1, the pattern is considered to be random (Clark & Evans, 1954, Mitchell, 2005). Mitochondria were first analyzed using the Analyze Particles command in Fiji to analyze and measure the individual mitochondria of a single cell. The NND plugin was then used to calculate the ANN of each individual mitochondrion.

### **3. Results**

*Arabidopsis* plants lacking a functional *FMT* gene show severe defects in mitochondrial distribution and movement, as well as deficits in root growth (El Zawily et al., 2014). Plants lacking a functional *FIS1A* gene have a reduction in the number of mitochondria per cell, as well as an increase in the size of individual mitochondria in protoplasts and leaves (Scott et al., 2006). How exactly *FMT* and *FIS1A* mediate these changes in mitochondria is still unclear. Given the role of mitochondria in the salt stress response, and given the fact that salt stress is sensed first in the soil by the roots, we wanted to examine the effects of a knockout of either *FMT* or *FIS1A*, as well as an overexpression of *FMT*, in mitochondria in the roots under both control and salt-stressed conditions. Additionally, since the effects of salt stress on mitochondrial morphology in wild type plants has not previously been characterized, we wanted to examine various mitochondrial parameters in the columella cells of the roots of wild type plants exposed to salt stress. These findings will further our understanding of the roles of *FMT* and *FIS1A* in mitochondrial morphology, as well as their role(s) in the salt stress response. In addition, it will provide insight into the effects of salt stress on mitochondrial morphology in wild type plants.

#### **3.1 Identification of the *FMT* and *FIS1A* genes**

The *FMT* gene was originally identified by Logan et al. (2003) and *fmt* mutants in *Arabidopsis* were shown to have an increased number of clustered mitochondria in the leaves. These mutants were further characterized by El Zawily et al. (2014), and were

found to have shorter roots, as well as an increase in the association time between mitochondria, as well as an increase in mitochondrial matrix mixing. The *FIS1A* gene was originally characterized by Scott et al. (2006), and *fis1A* mutants in *Arabidopsis* were found to have a reduced number of mitochondria per cell, but an increase in the size of individual mitochondria in protoplasts and leaves. However, the role of these genes with regards to whole-plant morphology, as well as their role in salt stress, has yet to be explored.

### **3.1.1 Expression levels of *FMT* and *FIS1A* in response to salt stress**

Expression levels of *FMT* and *FIS1A* under salt stress in the *Arabidopsis* root were examined using the *Arabidopsis* Spatio-Temporal Root Stress eFP Browser (<http://dinnenylab.info/browser/query>). This browser examines the expression levels of ~5 day old seedlings exposed to 140mM NaCl from 1 to 48 hours, compared to exposure on MS-Agar for 1 and 48 hours. A comparison of the expression levels of *FIS1A* and *FMT* to expression levels of the Salt Overly Sensitive genes (*SOS1*, *SOS2*, and *SOS3*), which are known to be induced by salt stress, is shown in Figure 2. It is clear that *FMT* gene expression increases sharply in as little as three hours in the epidermis, with a moderate increase in expression in the stele and cortex from 1-48 hours following NaCl exposure. *FIS1A* is only mildly upregulated in the epidermis in response to salt stress, similar to *SOS1* expression. *SOS2* has a moderate decrease in expression in the epidermis, stele, and cortex, while *SOS3* is initially highly upregulated from 1-3 hours, with an eventual decrease in expression after 48 hours. While this eFP Browser is informative for short-term exposure at 140mM NaCl, it does not provide information for

long-term exposure to NaCl stress at different concentrations. An in-depth phenotypic and functional analysis of both FMT and FIS1A under different salt-stressed conditions is therefore essential in furthering our understanding of the role of these genes during salt stress.

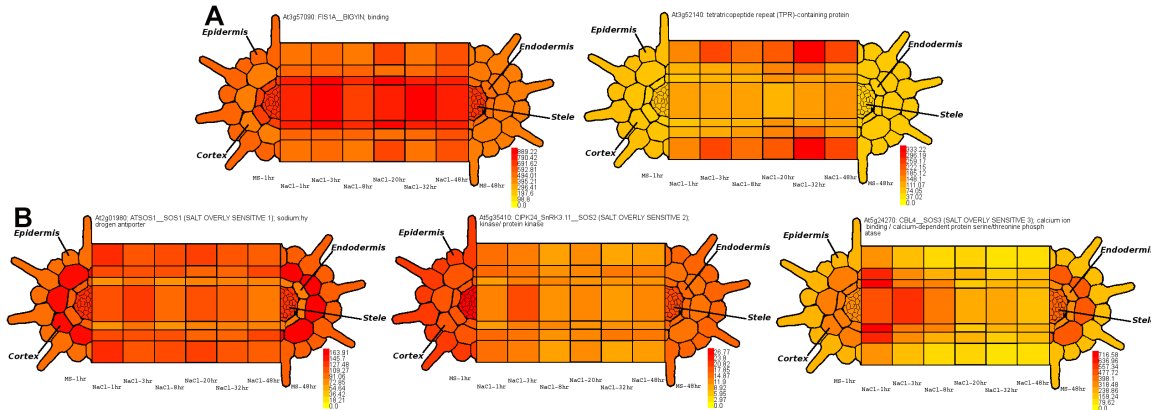


**Figure 2: Salt-regulated spatio-temporal expression in the *Arabidopsis* root.** A) FIS1A (left) and FMT (right). B) (left to right) SOS1, SOS2, SOS3.

### 3.2 Overexpression of the *FMT* gene in *Arabidopsis thaliana*

In order to further our understanding of the role of FMT in whole-plant and mitochondrial morphology, we created a transgenic *Arabidopsis* plant line (*FMT-OE*) overexpressing FMT under the control of the cauliflower mosaic virus (CaMV) 35S promoter. *Arabidopsis* plants were transformed with *Agrobacterium* containing the pFASTG02-FMT overexpression vector. The pFASTG02 vector carries a screenable marker that produces a GFP signal visible in the mature seed coat of transformed plants. Transgenic seeds from these plants were then sown to obtain T<sub>2</sub> seeds. Lines with a single transgene insertion were identified by an ~3:1 segregation ratio of GFP to no-GFP, respectively. Transgenic GFP seeds from these lines were sown to identify a

homozygous plant (FMT-3), which was identified by T<sub>3</sub> seed that exhibited 100% GFP fluorescence compared to WT seed (Fig. 3). Seeds from line FMT-3 were collected and used in subsequent experiments.

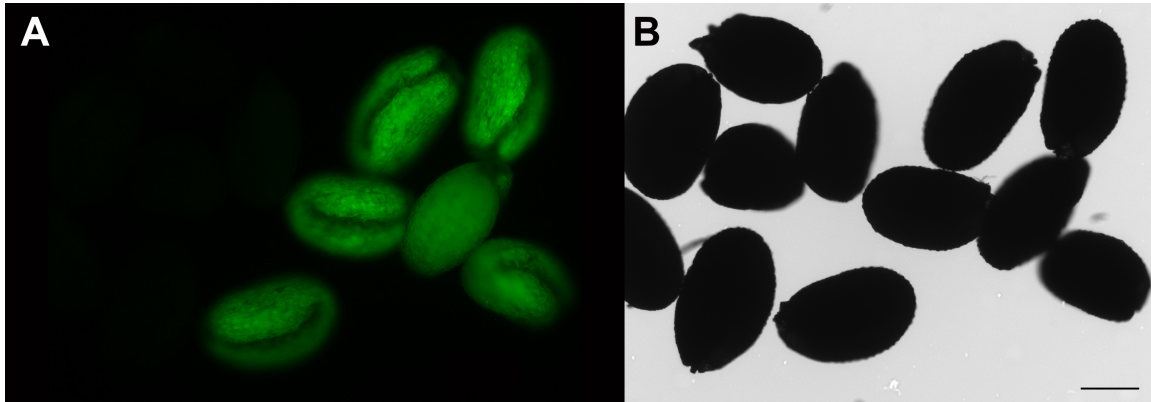


**Figure 3: Seeds of *Arabidopsis* plants transformed with pFASTG02-FMT give green fluorescence.**

A) (right) GFP-expressing T<sub>3</sub> generation seeds obtained from FMT-3, a homozygous *Arabidopsis* plant overexpressing the FMT gene in the pFASTG02 vector, (left) non-transformed WT seeds do not give green fluorescence. B) The same field view as in (A), but viewed under bright field light. Scale bar = 100  $\mu$ m.

### 3.3 Phenotypic analyses of the *fis1A*, *fnt*, and *FMT-OE* mutants

#### 3.3.1 *fis1A* mutants have shorter roots and slightly shorter leaves

As described above, a homozygous T-DNA insertion line for *FIS1A* (SALK\_006512C) was found within the SALK collection. When using primers spanning the insertion site, no transcript could be detected via PCR. The T-DNA insertion hypothetically leads to a block of transcription, rendering a truncated or non-functional FIS1A protein.

Under control conditions, *fis1A* mutant plants did not have a significantly different germination rate compared to WT plants (98.6%  $\pm$ 3.26% versus 99.2%  $\pm$ 1.88%, respectively) (Fig. 4A), nor did they take longer to germinate than WT plants (1.5 days

$\pm 0.51$  days versus  $1.24$  days  $\pm 0.43$  days, respectively) (Fig. 4B). Leaf length was not significantly ( $p=0.0775$ ) shorter in *fis1A* mutants compared to the WT ( $1.03$  cm  $\pm 0.21$  cm versus  $1.23$   $\pm 0.25$  cm, respectively) (Figs. 4C, 5N). These mutants also did not display differences in days to flowering ( $29.4$  days  $\pm 1.99$  days) compared to the WT ( $28.89$  days  $\pm 1.28$  days) (Fig. 4D). However, *fis1A* mutants did display significantly shorter roots at both 7 ( $0.59$  cm  $\pm 0.17$  cm) and 14 ( $0.85$  cm  $\pm 0.43$  cm) days old under control conditions compared to the WT ( $0.86$  cm  $\pm 0.27$  cm and  $1.56$  cm  $\pm 0.48$  cm, respectively) (Figs. 4E,F, 5B,F).

### **3.3.2 *fmt* mutants have shorter roots and leaves and take longer to flower**

As described above, a homozygous T-DNA insertion line for *FMT* (SALK\_046271C) was found within the SALK collection. When using primers spanning the insertion site, no transcript could be detected via PCR. The T-DNA insertion hypothetically leads to a block of transcription, rendering a truncated or non-functional FMT protein.

Under control conditions, *fmt* mutant plants did not have a significantly different germination rate ( $98.6\% \pm 3.13\%$ ) (Fig. 4A) nor did they take longer to germinate ( $1.33$  days  $\pm 0.48$  days) compared to WT plants (Fig. 4B). However, leaf length was significantly shorter in *fmt* mutants ( $0.93$  cm  $\pm 0.20$  cm) (Fig. 4C, 5O), and these mutants also took significantly longer to flower ( $33.57$  days  $\pm 2.82$  days) compared to the WT (Fig. 4D). *fmt* mutants also displayed significantly shorter roots at both 7 ( $0.54$  cm  $\pm 0.18$  cm) and 14 ( $0.85$  cm  $\pm 0.33$  cm) days old under control conditions compared to the WT (Fig. 4E,F, 5C,G).

### **3.3.3 *FMT-OE* mutants have a lower rate of germination, take longer to germinate, and have shorter roots and leaves**

Under control conditions, *FMT-OE* mutant plants had a much lower rate of germination, at only  $82.33\% \pm 9.77\%$  (Fig. 4A). These plants also took longer to germinate (3.12 days  $\pm 0.64$  days) compared to WT, *fis1A*, and *fnt* plants (Fig. 4B). Despite this delayed germination, these mutants did not take longer to flower (29.83 days  $\pm 1.16$  days) compared to the WT (Fig. 4D). Similar to *fnt* mutants, leaf length was significantly shorter in *FMT-OE* mutants (0.90 cm  $\pm 0.26$  cm) versus the WT (Fig. 4C, 5P). Interestingly, *FMT-OE* mutants displayed significantly shorter roots at 7 days old (0.21 cm  $\pm 0.10$  cm), but not at 14 days old (1.25 cm  $\pm 0.51$  cm) under control conditions compared to the WT (Fig. 4E,F, 5D, H).

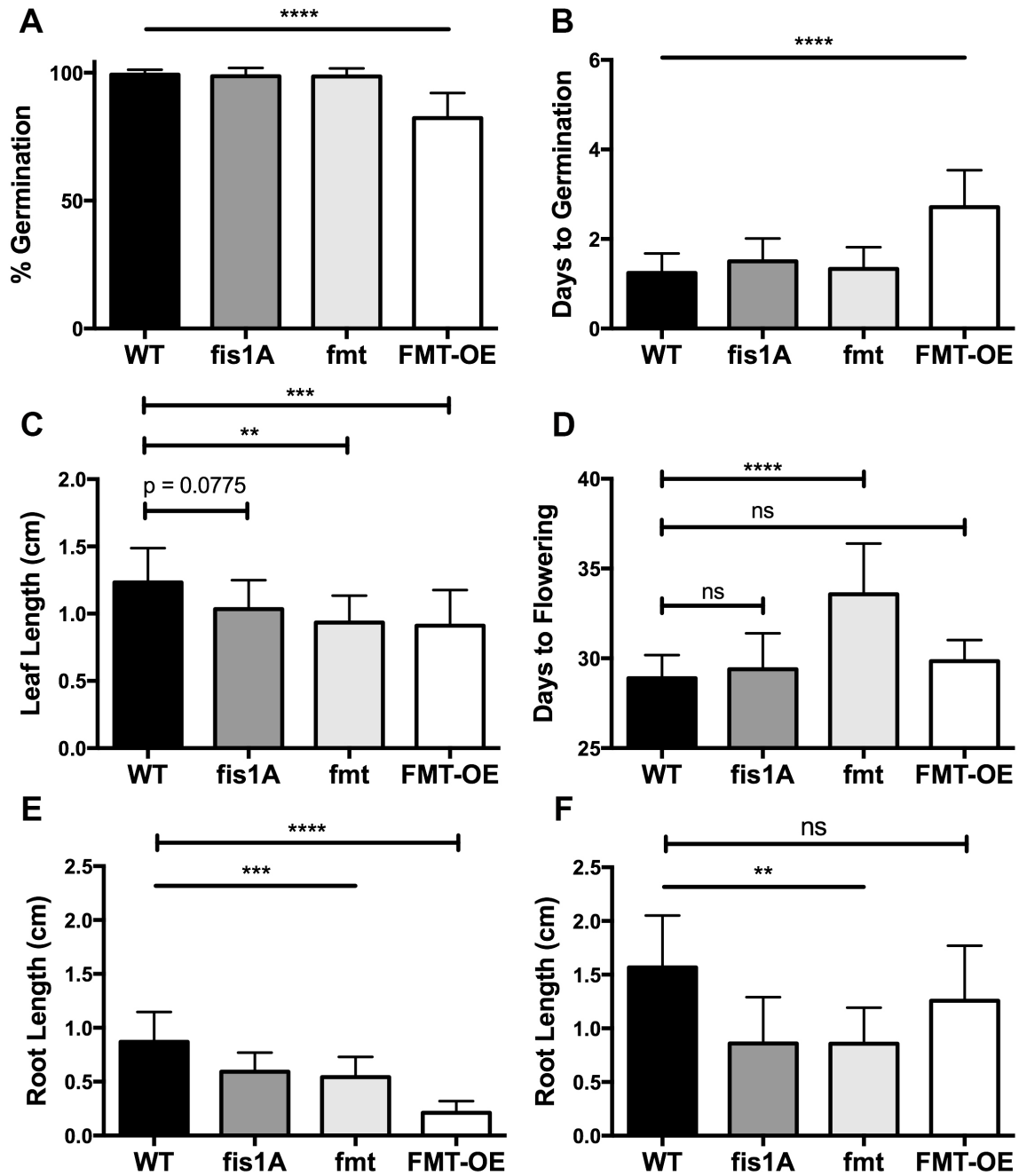


**Figure 4: Phenotypic differences between WT, *fis1A*, *fmt*, and *FMT-OE* lines under control conditions.** A) % Germination, B) Days to germination, C) Leaf length, D) Days to flowering, E) Root length at 7 days old, F) Root length at 14 days old. Statistical analysis indicates significant differences (\*\*\*\*,  $P \leq 0.0001$ , \*\*\*  $P \leq 0.001$ , \*\*  $P \leq 0.01$ , ns = not significant,  $P > 0.05$ ) compared with controls using one-way ANOVA.

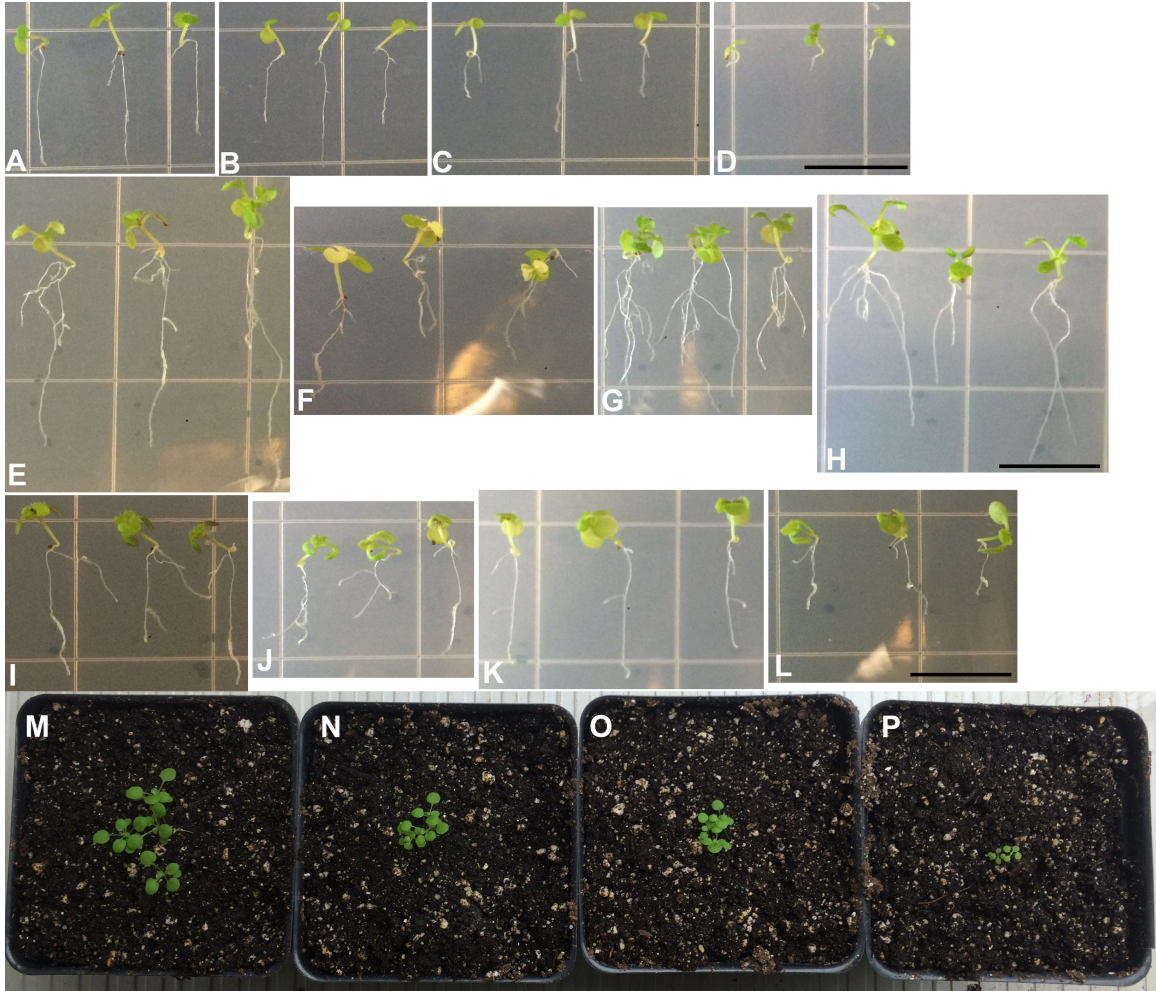


**Figure 5: Visualization of phenotypic differences between WT, *fis1A* *fmt*, and *FMT-OE* lines under control and salt-stressed conditions.** A-D) *Arabidopsis* seedlings at 7 days old under control conditions on MS-Agar plates. A) WT, B) *fis1A*, C) *fmt*, D) *FMT-OE*. E-H) *Arabidopsis* seedlings at 14 days old under control conditions on MS-Agar plates. E) WT, F) *fis1A*, G) *fmt*, H) *FMT-OE*. I-L) *Arabidopsis* seedlings at 14 days old under salt-stressed conditions on 125mM NaCl MS-Agar plates. I) WT, J) *fis1A*, K) *fmt*, L) *FMT-OE*. M-P) *Arabidopsis* seedlings at 7 days old under control conditions in the soil. M) WT, N) *fis1A*, O) *fmt*, P) *FMT-OE*. Scale bar = 1 cm.

### 3.4 Effects of salt stress on *fis1A*, *fmt*, and *FMT-OE* mutants and WT plants

In order to examine the role of the FIS1A and FMT mitochondrial proteins in response to salt stress, *fis1A*, *fmt*, and *FMT-OE* mutants were exposed to either 125mM NaCl stress on MS-Agar media, or gradual salt stress ranging from 50-140mM NaCl in the soil. Additionally, to examine the effects of salt stress on WT *Arabidopsis* plants, and to serve as a control, these plants were also exposed to salt stress on plates and in the soil. On 125mM NaCl MS-Agar plates, WT plants did not have a significant difference in percent germination (Fig. 6A), but took longer to germinate compared to control conditions (3.64 days  $\pm$ 0.43 days compared to 1.24 days  $\pm$ 0.43 days, respectively) (Fig. 6B). These plants also had significantly shorter roots compared to WT plants under control conditions (0.99 cm  $\pm$ 0.33 cm compared to 1.56 cm  $\pm$ 0.48 cm, respectively) (Fig. 6E, 5I). Under salt-stressed conditions in the soil, WT leaves were significantly shorter compared to the WT control (0.90 cm  $\pm$ 0.15 cm compared to 1.23 cm  $\pm$ 0.25 cm, respectively) (Fig. 6C), and these plants took significantly longer to flower compared to WT plants under control conditions (31.37 days  $\pm$ 2.21 days compared to 28.89 days  $\pm$ 1.28 days, respectively) (Fig. 6D).

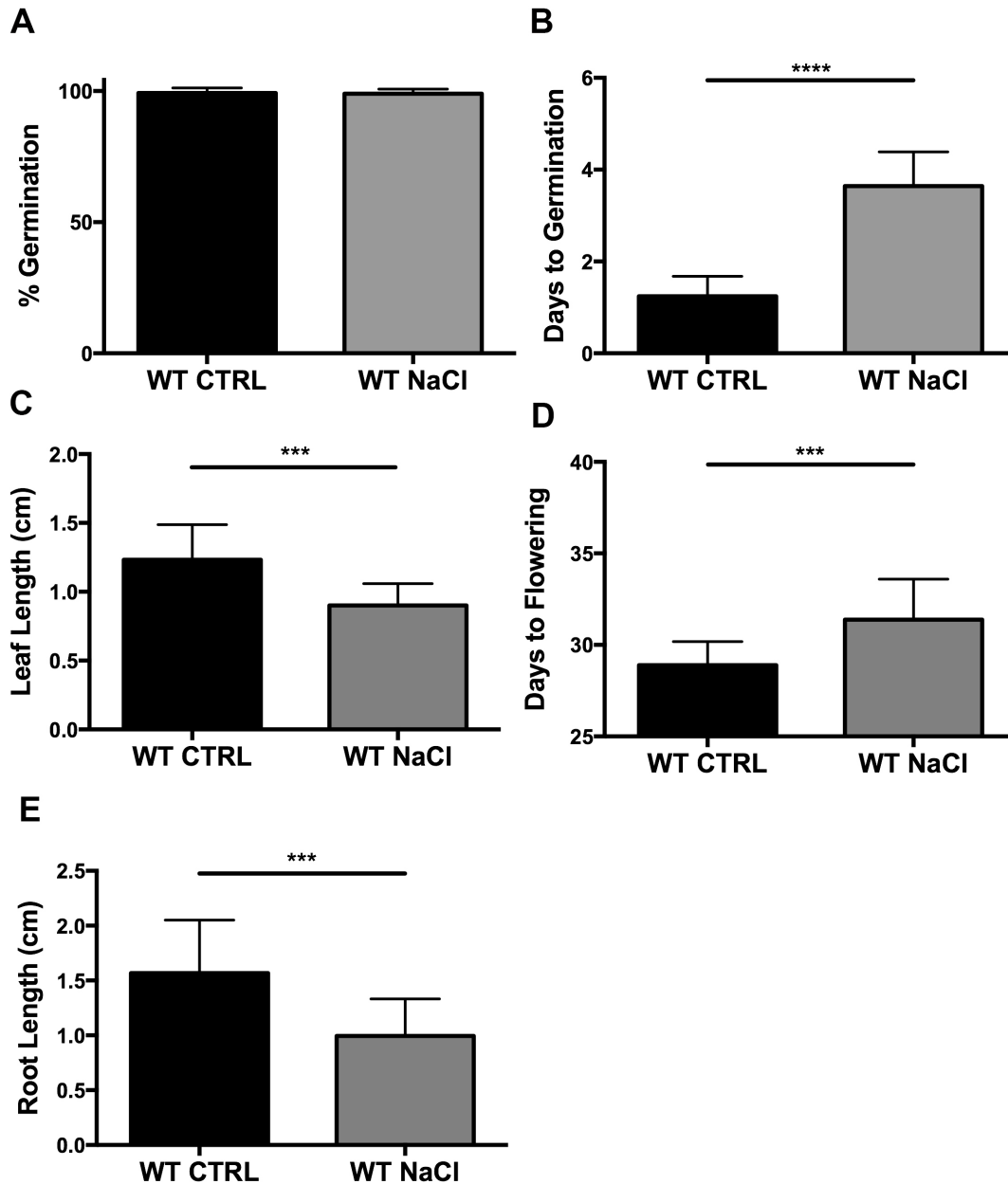


**Figure 6: Salt stress affects days to germination and flowering, as well as leaf and root length in wild type *Arabidopsis*.** A) % Germination, B) Days to germination, C) Leaf length, D) Days to flowering, E) Root length at 14 days old. Black bars indicate control conditions, grey bars indicate salt-stressed conditions. Statistical analysis indicates significant differences (\*\*\*\*,  $P \leq 0.0001$ , \*\*\*,  $P \leq 0.001$ ) compared with controls using two-tailed Student's *t* test.

On 125mM NaCl MS-Agar plates, *fis1A* mutants germinated at relatively the same rate compared to control conditions (96.5%  $\pm$ 4.94% compared to 98.66%  $\pm$ 3.26%, respectively) (Fig. 7A), however these plants took longer to germinate compared to control conditions (3.84 days  $\pm$ 0.80 days compared to 1.5 days  $\pm$ 0.51 days, respectively) (Fig. 7B). These plants also had significantly shorter roots compared to *fis1A* plants under control conditions (0.64 cm  $\pm$ 0.25 cm compared to 0.85 cm  $\pm$ 0.43 cm, respectively) (Fig. 7E, 5J). Under salt stress conditions in the soil, *fis1A* leaves were significantly shorter compared to controls (0.82 cm  $\pm$ 0.13 cm compared to 1.03 cm  $\pm$ 0.21 cm, respectively) (Fig.7C), and these plants took significantly longer to flower compared to controls (34.31 days  $\pm$ 2.96 days compared to 29.4 days  $\pm$ 1.99 days, respectively) (Fig. 7D).

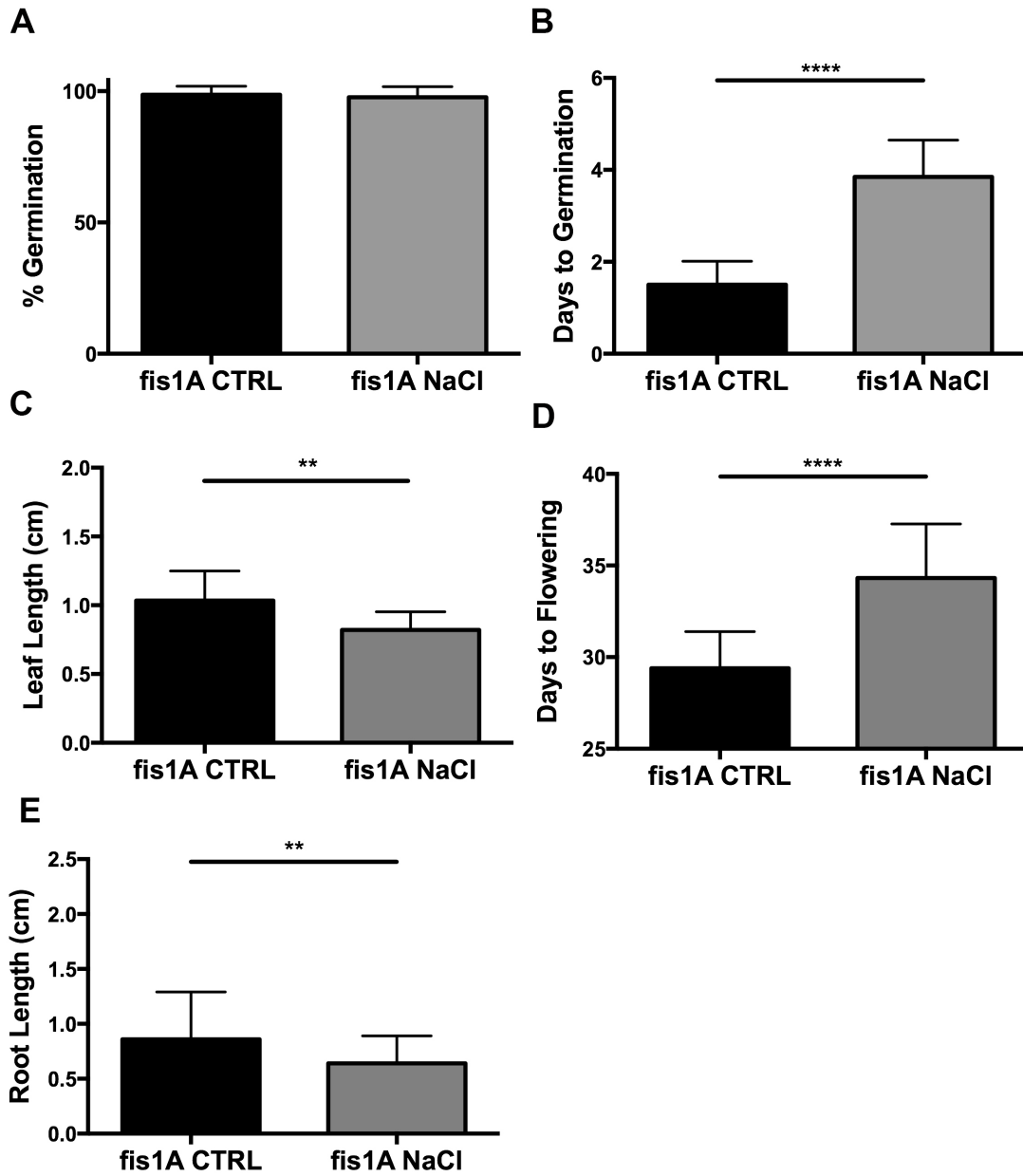


**Figure 7: Salt stress affects days to germination and flowering, as well as leaf and root length in *fis1A* mutants.** A) % Germination, B) Days to germination, C) Leaf length, D) Days to flowering, E) Root length at 14 days old. Black bars indicate control conditions, grey bars indicate salt-stressed conditions. Statistical analysis indicates significant differences (\*\*\*\*,  $P \leq 0.0001$ , \*\*,  $P \leq 0.01$ ) compared with controls using two-tailed Student's *t* test.

Compared to WT plants under salt-stressed conditions, salt-stressed *fis1A* mutant plants did not have a significantly different germination rate (Fig. 8A), nor did they take longer to germinate (Fig. 8B). These mutants also did not have significantly shorter roots at 14 days old compared to the WT under the same conditions (Fig. 8E). Under salt-stressed conditions in the soil, the leaf length of *fis1A* mutants was not significantly shorter compared to WT plants under the same conditions (Fig. 8C), although the number of days to flowering was significantly increased (Fig. 8D).

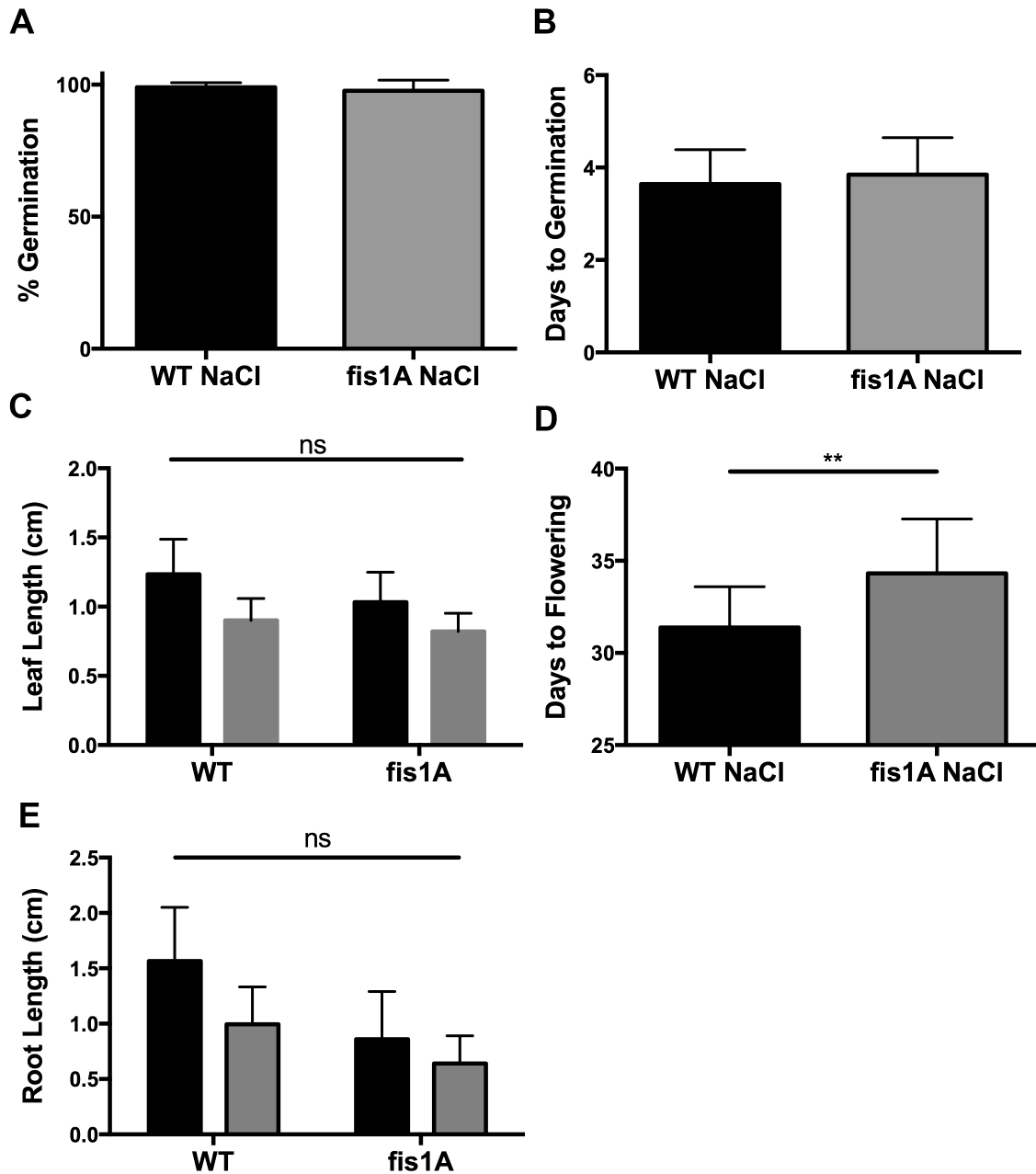


**Figure 8: Days to flowering is increased in *fis1A* mutants compared to the WT under salt-stressed conditions.** A) % Germination, B) Days to germination, C) Leaf length, D) Days to flowering, E) Root length at 14 days old. Black bars indicate control conditions, grey bars indicate salt-stressed conditions. Statistical analysis indicates significant differences (\*\*,  $P \leq 0.01$ , ns = not significant,  $P > 0.05$ ) compared with controls using two-tailed Student's *t* test (A, B, C) or two-way ANOVA (C, E).

On 125mM NaCl MS-Agar plates, *fmt* mutants germinated at the same rate compared to control conditions (98.25%  $\pm$ 2.36% compared to 98.6%  $\pm$ 3.13%, respectively) (Fig. 9A), however these plants took much longer to germinate compared to controls (3.84 days  $\pm$ 0.98 days compared to 1.3 days  $\pm$ 0.48 days, respectively) (Fig. 9B). These plants did not have significantly shorter roots compared to *fmt* plants under control conditions (0.75 cm  $\pm$ 0.28 cm compared to 0.85 cm  $\pm$ 0.33 cm, respectively) (Fig. 9E, 7K). Under salt stress conditions in the soil, the leaves of *fmt* mutants were not significantly shorter compared to controls (0.83 cm  $\pm$ 0.16 cm compared to 0.93 cm  $\pm$ 0.20 cm, respectively) (Fig. 9C), nor did these plants take longer to flower compared to controls (33.42 days  $\pm$ 3.24 days compared to 33.57 days  $\pm$ 2.82 days, respectively) (Fig. 9D).

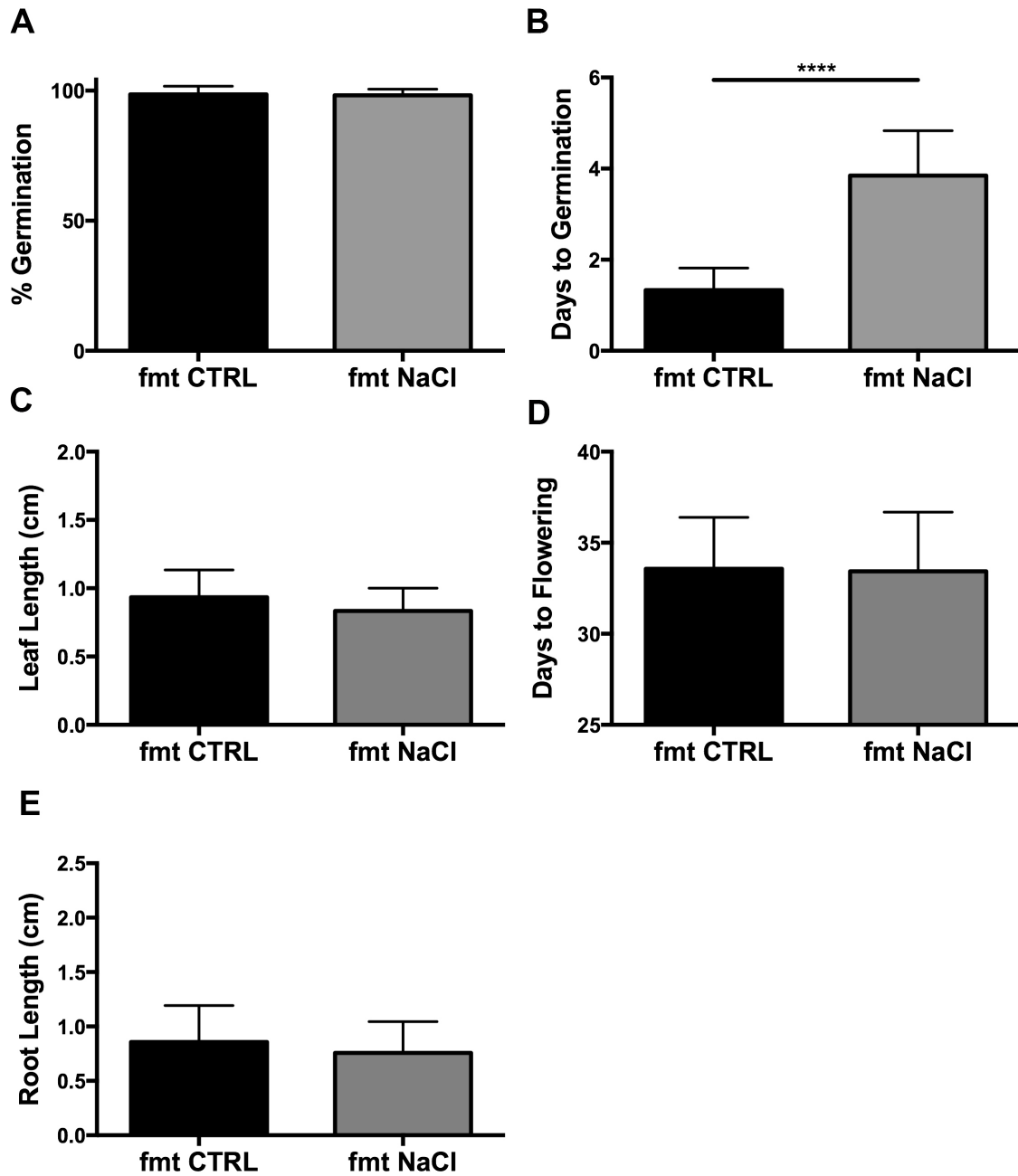


**Figure 9: Salt stress affects days to germination in *fmt* mutants.** A) % Germination, B) Days to germination, C) Leaf length, D) Days to flowering, E) Root length at 14 days old. Black bars indicate control conditions, grey bars indicate salt-stressed conditions. . Statistical analysis indicates significant differences (\*\*\*\*,  $P \leq 0.0001$ ) compared with controls using two-tailed Student's *t* test.

Compared to WT plants under salt-stressed conditions, *fmt* mutant plants did not have a significantly different germination rate, nor did they take longer to germinate (Fig. 10A,B). These mutants also had shorter roots, although it was not statistically significant ( $P= 0.0605$ ) (Fig. 10E). However, under salt-stressed conditions in the soil, leaves of *fmt* mutants were significantly shorter and days to flowering was significantly longer compared to WT plants under the same conditions (Fig. 10C,D).

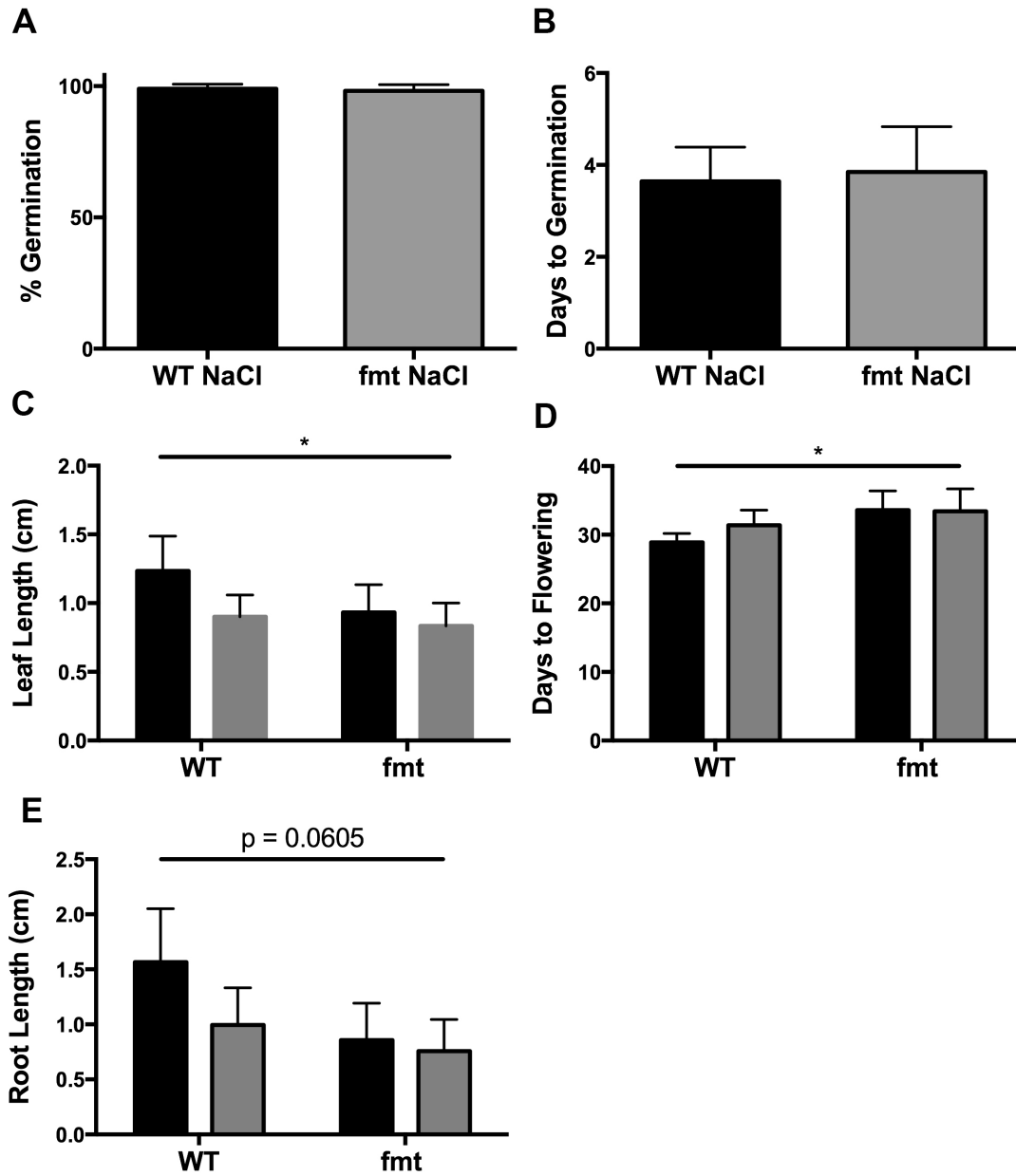


**Figure 10: Days to flowering is increased and root and leaf length are decreased in *fmt* mutants compared to the WT under salt-stressed conditions.** A) % Germination, B) Days to germination, C) Leaf length, D) Days to flowering, E) Root length at 14 days old. Black bars indicate control conditions, grey bars indicate salt-stressed conditions. Statistical analysis indicates significant differences (\*,  $P \leq 0.05$ ) compared with controls using two-tailed Student's *t* test (A, B) or two-way ANOVA (C, D, E).

On 125mM NaCl MS-Agar plates, the percent germination of *FMT-OE* mutants decreased further compared to *FMT-OE* seedlings under control conditions ( $57.5\% \pm 3.53\%$  compared to  $82.33\% \pm 9.77\%$ , respectively) (Fig. 11A). Days to germination increased significantly compared to controls (4.46 days  $\pm 1.12$  days compared to 2.71 days  $\pm 0.82$  days, respectively) (Fig. 11B). These plants also had significantly shorter roots compared to *FMT-OE* plants under control conditions (0.53 cm  $\pm 0.11$  cm compared to 1.25 cm  $\pm 0.51$  cm, respectively) (Fig. 11E, 5L). Under salt-stressed conditions in the soil, the leaves of *FMT-OE* mutants were significantly shorter compared to *FMT-OE* plants under control conditions (0.65 cm  $\pm 0.14$  cm compared to 0.90 cm  $\pm 0.26$  cm, respectively) (Fig. 11C). However, these plants did not take longer to flower compared to controls (31.9 days  $\pm 3.03$  days compared to 29.83 days  $\pm 1.16$  days, respectively) (Fig. 11D).

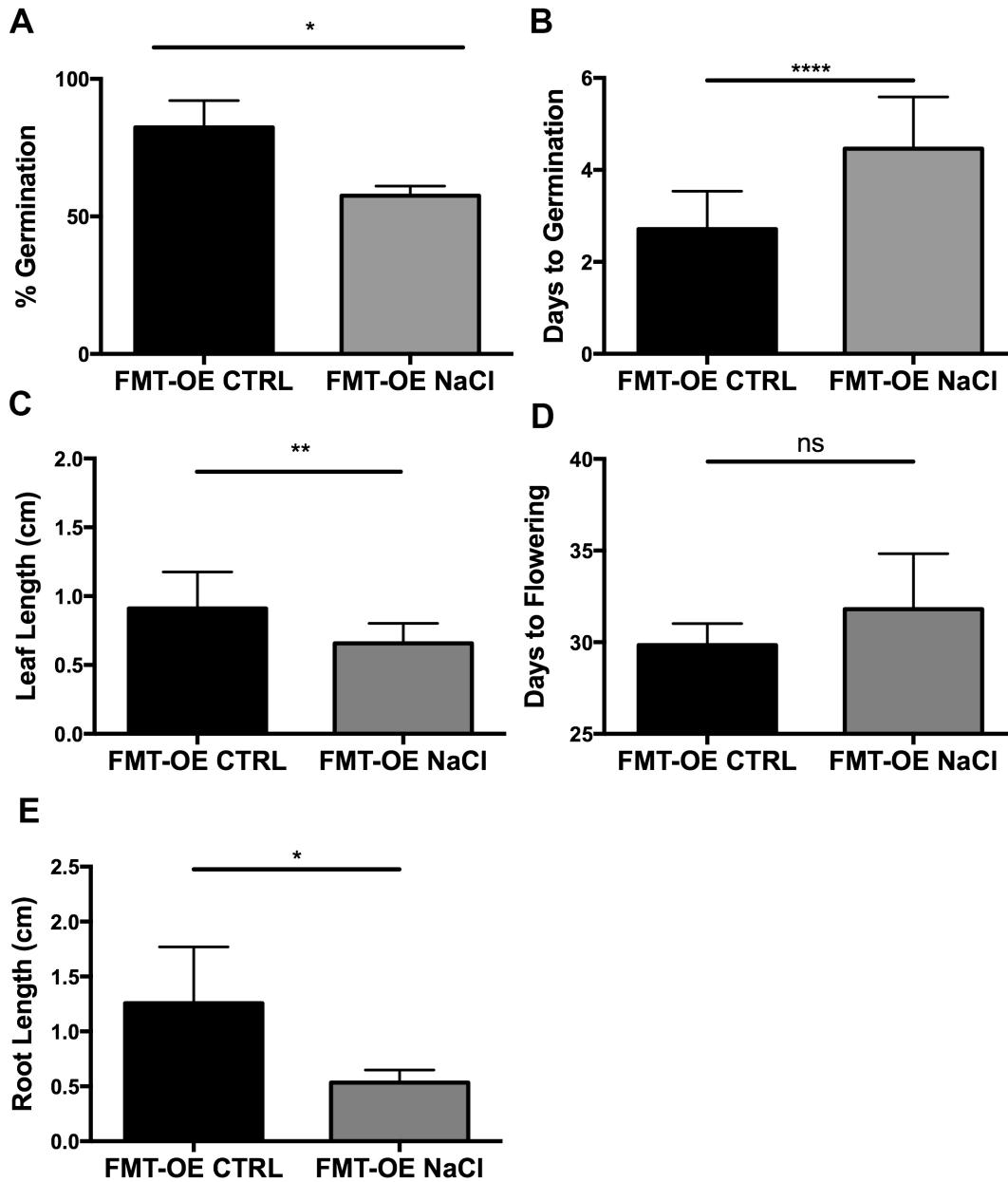


**Figure 11: Salt stress affects percent germination, days to germination, and leaf and root length in *FMT-OE* mutants.** A) % Germination, B) Days to germination, C) Leaf length, D) Days to flowering, E) Root length. Black bars indicate control conditions, grey bars indicate salt-stressed conditions. Statistical analysis indicates significant differences (\*\*\*\*,  $P \leq 0.0001$ , \*\*,  $P \leq 0.01$ , \*,  $P \leq 0.05$ , ns = not significant,  $P > 0.05$ ) compared with controls using two-tailed Student's *t* test.

Compared to WT plants under salt-stressed conditions, salt-stressed *FMT-OE* mutants had a significantly decreased germination rate (Fig. 12A), and a difference in days to germination approached significance ( $p=0.0739$ ) (Fig. 12B). Root length was also significantly shorter (Fig. 12E). Under salt-stressed conditions in the soil, neither the length of the leaves nor the days to flowering were significantly different in *FMT-OE* mutants compared to WT plants under the same conditions (Fig. 12D).

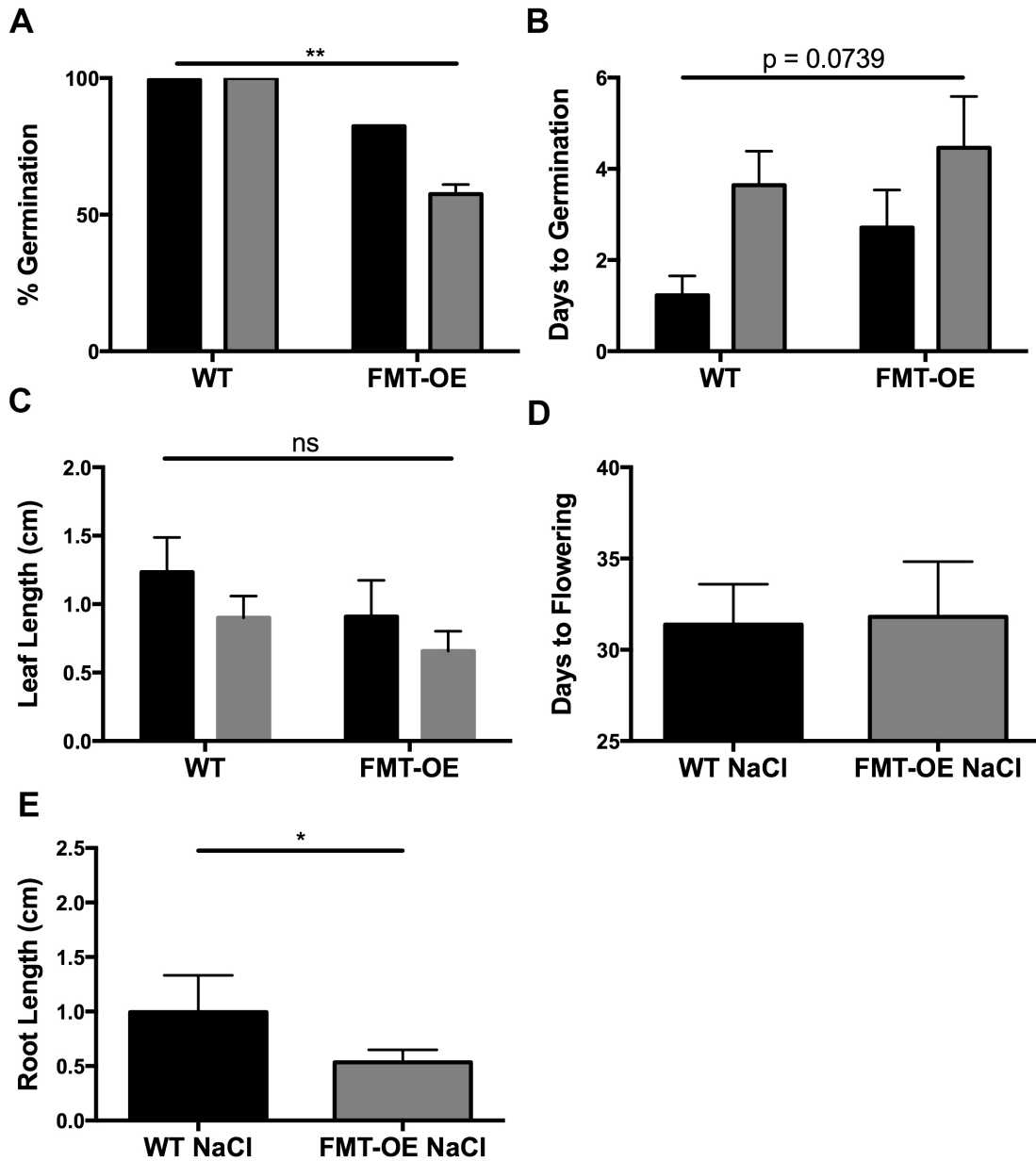


**Figure 12: Germination percentage and root length are decreased in *FMT-OE* mutants compared to the WT under salt-stressed conditions.** A) % Germination, B) Days to germination, C) Leaf length, D) Days to flowering, E) Root length at 14 days old. Black bars indicate control conditions, grey bars indicate salt-stressed conditions. Statistical analysis indicates significant differences (\*\*,  $P \leq 0.01$ , \*,  $P \leq 0.05$ , ns = not significant,  $P > 0.05$ ) compared with controls using two-tailed Student's *t* test (D,E) or two-way ANOVA (A,B,C).

### 3.5 Electron microscopy analysis of WT, *fis1A*, *fmt*, and *FMT-OE* plants

Mitochondria are known to play an integral role in the salt stress response. One response to salt stress is salt-avoidance gravitropism, in which amyloplasts from the root cap are degraded, and auxin is asymmetrically distributed via PIN2 transport, in order to induce root bending. The mitochondrial FMT protein is known to be upregulated during salt stress, and *fmt* mutants were shown to have significantly decreased root cap/meristematic zones in their roots (El Zawily et al., 2014). Thus, an analysis of the mitochondria in the root cap of *fmt* mutants would provide insight into the role of this gene in root cap morphology and the salt stress response. Furthermore, an analysis of the root cells of another mitochondrial mutant, *fis1A*, as well as *FMT-OE* mutants, would provide further insight into the role of mitochondria in the root. Thus, we performed an electron microscopy analysis of mitochondria in columella cells in *fis1A*, *fmt*, and *FMT-OE* mutants and compared these results to WT plants under both control and salt-stressed conditions.

Electron microscopy analysis of the columella cells in the roots of WT, *fis1A*, *fmt*, and *FMT-OE* plants under control conditions revealed major differences in the number of mitochondria per cell, mitochondrial coverage, and mitochondrial clustering (Fig. 13). The wide variation in mitochondrial area ( $<0.1 \mu\text{m}^2$  to  $>0.6 \mu\text{m}^2$ ) did not reveal any significant differences between the three mutant plants compared to the WT (Fig. 14A). WT plants had an average mitochondrial area of  $0.276 \mu\text{m}^2 \pm 0.15 \mu\text{m}^2$ , *fis1A* mutants had an average mitochondrial area of  $0.279 \mu\text{m}^2 \pm 0.16 \mu\text{m}^2$ , *fmt* mutants had an average mitochondrial area of  $0.279 \mu\text{m}^2 \pm 0.14 \mu\text{m}^2$ , and *FMT-OE* mutants had an average mitochondrial area of  $0.298 \mu\text{m}^2 \pm 0.15 \mu\text{m}^2$ . *fis1A* mutants did not display a significant

difference in mitochondrial AR (average  $1.70 \pm 0.05$ ), nor did *fmt* mutant plants (average  $1.56 \pm 0.13$ ), or *FMT-OE* mutants (average  $1.85 \pm 0.13$ ) compared to WT plants (average  $1.71 \pm 0.05$ ) (Fig. 14B). *fmt* mutant plants had a significantly increased average number of mitochondria per cell ( $20.86 \pm 13.19$ ) compared to the WT ( $9.21 \pm 3.21$ ), *fis1A* ( $13.06 \pm 4.28$ ), and *FMT-OE* plants ( $14.23 \pm 8.15$ ) (Fig. 14C). Both *fis1A* and *fmt* plants had increased mitochondrial coverage ( $15.92\% \pm 8.15\%$  and  $16.34\% \pm 9.31\%$ , respectively), compared to the WT ( $7.36\% \pm 2.33\%$ ) and *FMT-OE* plants ( $11.13\% \pm 5.49\%$ ) (Fig. 14D).

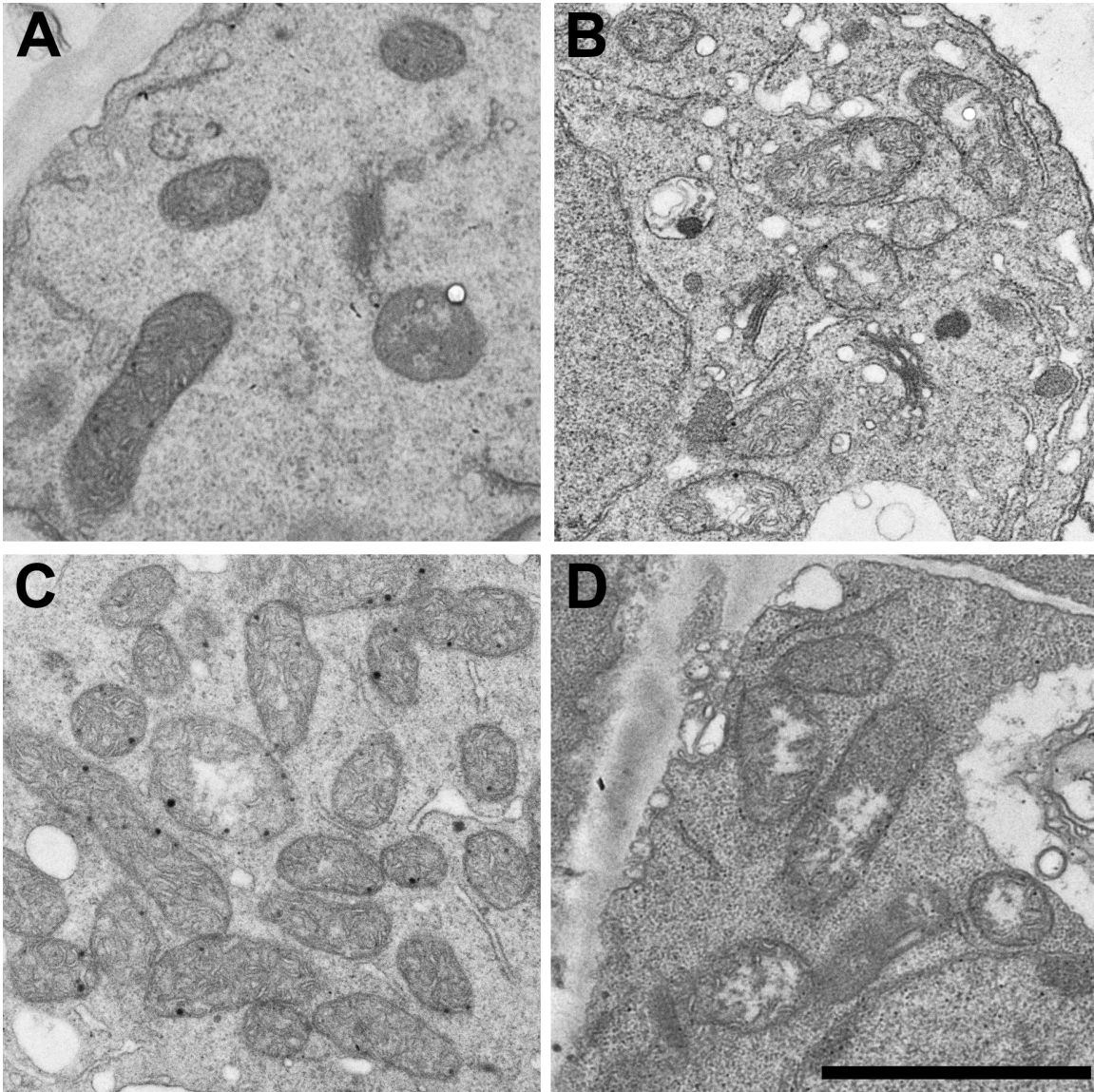


**Figure 13: Differences in mitochondria between WT, *fis1A*, *fmt*, and *FMT-OE* lines under control conditions.** A) WT, B) *fis1A*, C) *fmt*, D) *FMT-OE*. Each square represents a 4  $\mu\text{m}$  x 4  $\mu\text{m}$  area selected from a representative cell from each genotype. Scale bar = 2  $\mu\text{m}$ .

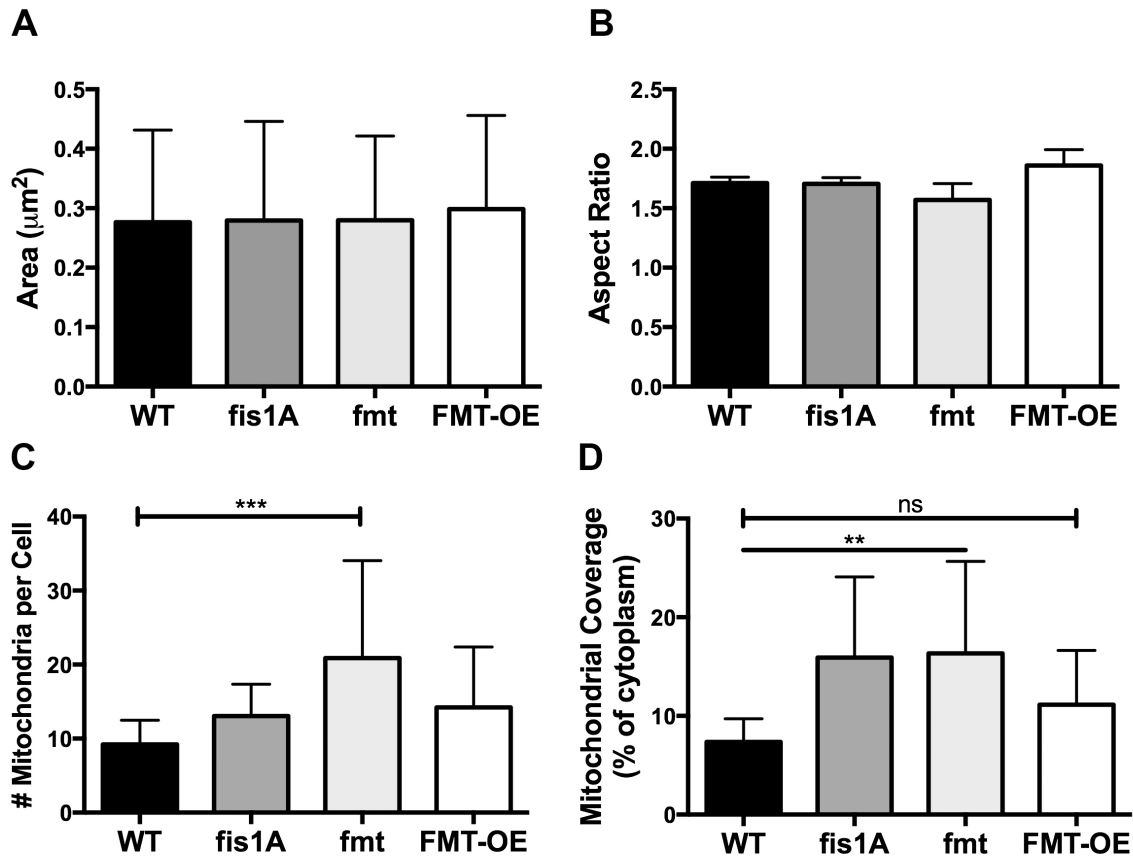


**Figure 14: Comparison of various mitochondrial parameters between WT, *fis1A*, *fmt*, and FMT-OE lines.** A) Mitochondrial area, B) Mitochondrial aspect ratio, C) # of mitochondria per cell, D) Mitochondrial coverage as a % of cytoplasm. Statistical analysis indicates significant differences (\*\*\*,  $P \leq 0.001$ , \*\*,  $P \leq 0.01$ , ns = not significant,  $P > 0.05$ ) compared with controls using one-way ANOVA.

### 3.5.1 Salt stress affects various mitochondrial parameters in WT, *fis1A*, and *fmt*

Electron microscopy analysis of the columella cells in the roots of WT, *fis1A*, and *fmt* plants under salt-stressed conditions revealed major changes in mitochondrial area, number of mitochondria per cell, mitochondrial coverage, and mitochondrial clustering (Figs. 15, 16). Under 125mM NaCl salt-stressed conditions, the average mitochondrial area ( $0.177 \mu\text{m}^2 \pm 0.09 \mu\text{m}^2$ ) decreased significantly in the WT compared to control conditions (Fig. 17A,B), although AR did not differ significantly ( $1.56 \pm 0.09$ ). Both the average number of mitochondria per cell ( $39.83 \pm 14.82$ ) and mitochondrial coverage

(12.88%  $\pm$ 0.98%), increased significantly (Fig. 17C,D). In *fis1A* mutants, the average mitochondrial area (0.169  $\mu\text{m}^2$   $\pm$ 0.08  $\mu\text{m}^2$ ) decreased significantly, although AR did not (1.59  $\pm$ 0.05) (Fig. 18A,B). The average number of mitochondria per cell (24.33  $\pm$ 12.29) was significantly increased, while mitochondrial coverage was significantly decreased (6.52%  $\pm$ 1.36%) (Fig. 18C,D). Mitochondria in *fmt* plants were significantly smaller (0.219  $\mu\text{m}^2$   $\pm$ 0.07  $\mu\text{m}^2$ ), however, aspect ratio (1.48  $\pm$ 0.03), the average number of mitochondria per cell (22.85  $\pm$ 7.35), and total mitochondrial coverage (17.34%  $\pm$ 6.45%) did not change significantly compared to control conditions (Fig. 19 A,B,C,D).

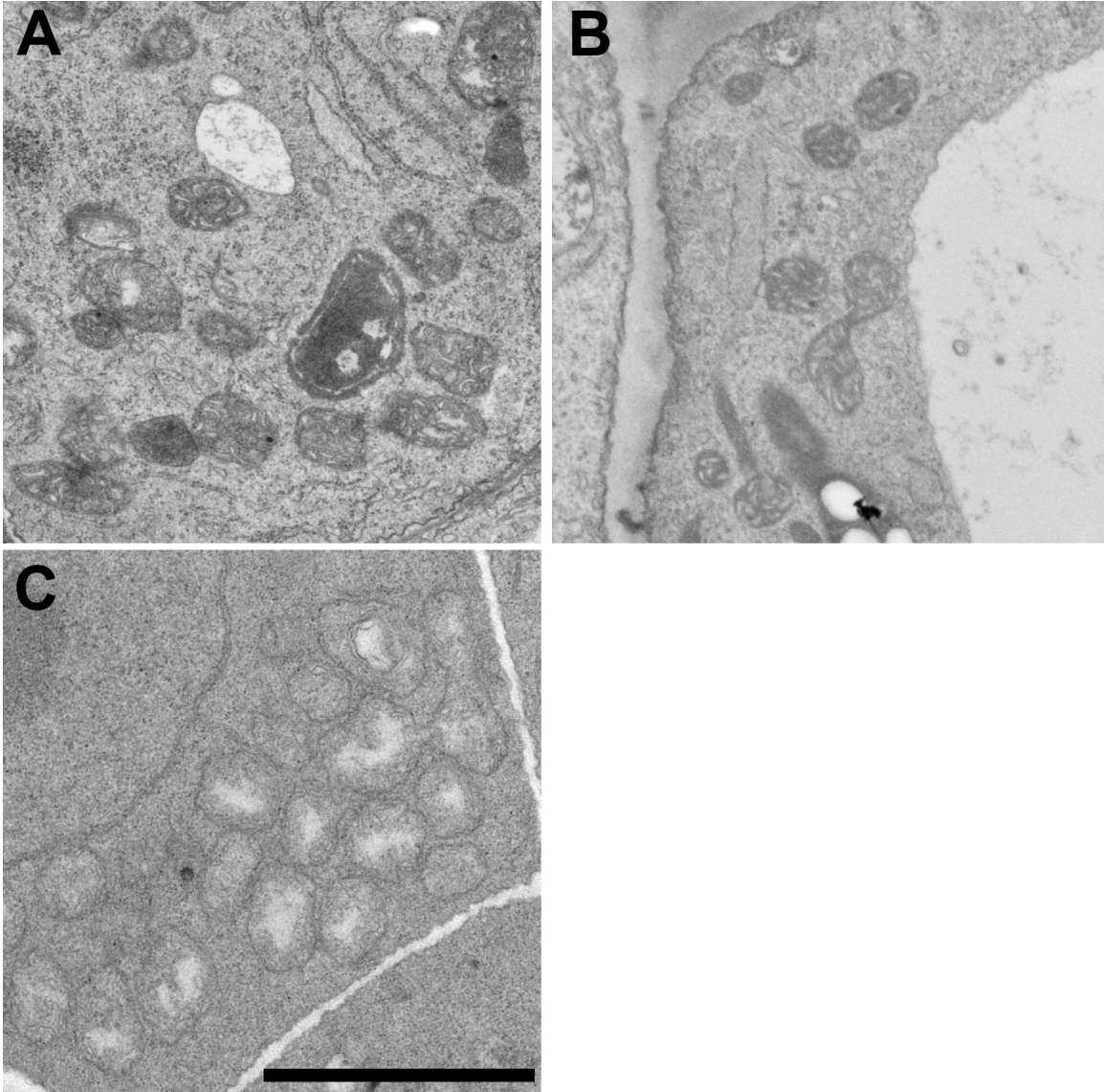


**Figure 15: Differences in mitochondria between WT, *fis1A*, and *fmt* lines under salt stress.** A) WT. B) *fis1A*. C) *fmt*. Each square represents a 4  $\mu\text{m}$  x 4  $\mu\text{m}$  area selected from a representative cell from each genotype. Scale bar = 2  $\mu\text{m}$ .

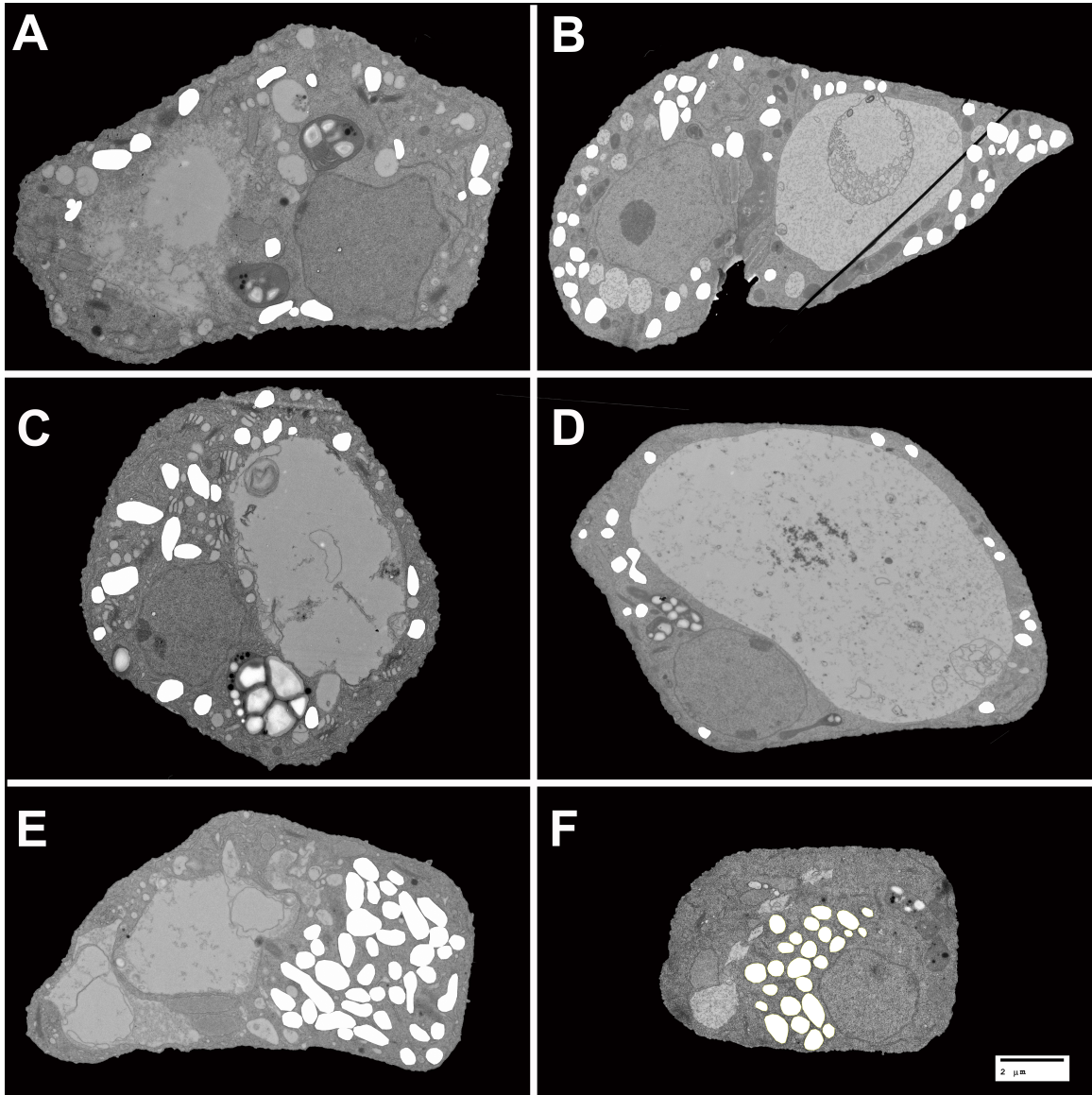


**Figure 16: Visualization of the effects of salt stress on WT, *fis1A*, and *fnt* lines.** A) WT under control conditions, B) WT under salt-stressed conditions, C) *fis1A* under control conditions, D) *fis1A* under salt-stressed conditions, E) *fnt* under control conditions, F) *fnt* under salt-stressed conditions. Mitochondria are shown filled in white. Scale bar = 2  $\mu\text{m}$ .

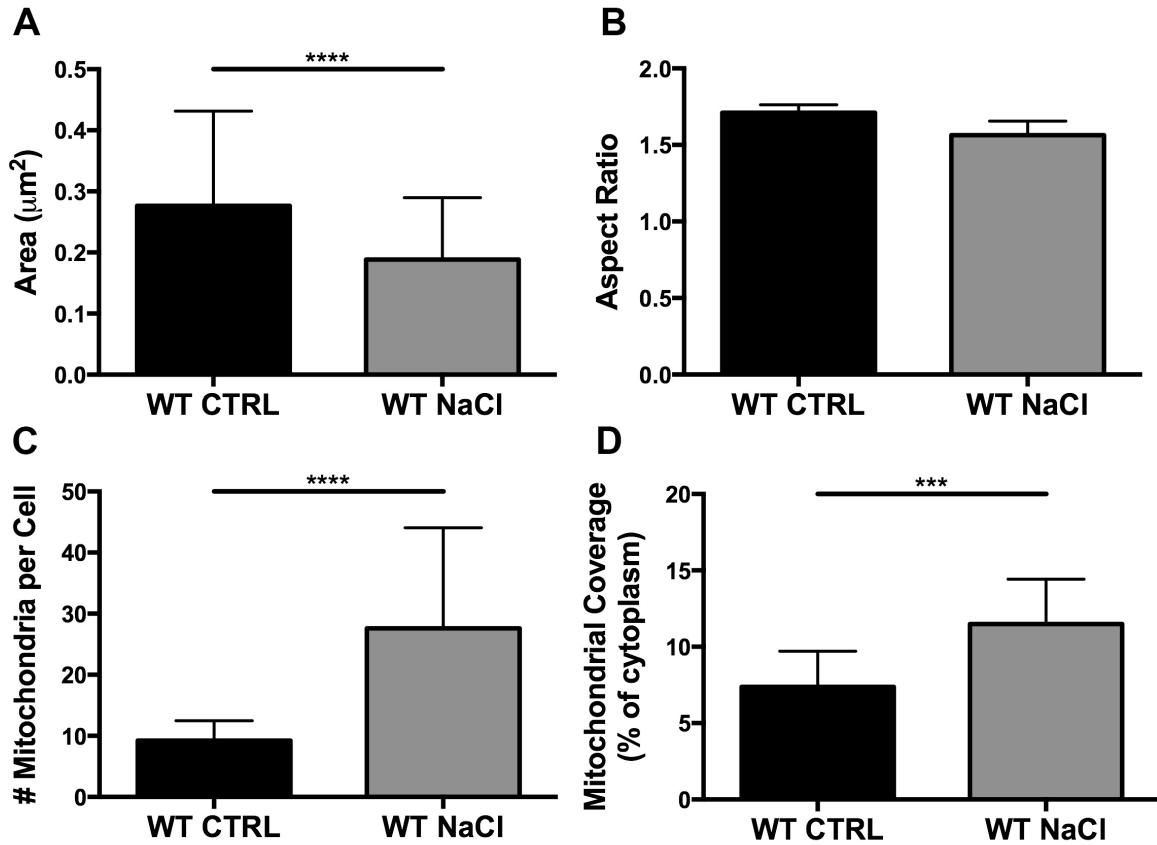


**Figure 17: Comparison of various mitochondrial parameters between WT plants under control and salt-stressed conditions.** A) Mitochondrial area, B) Mitochondrial aspect ratio, C) # of mitochondria per cell, D) Mitochondrial coverage as a % of cytoplasm. Statistical analysis indicates significant differences (\*\*\*\*,  $P \leq 0.0001$ , \*\*\*,  $P \leq 0.001$ ) compared with controls using one-way ANOVA.

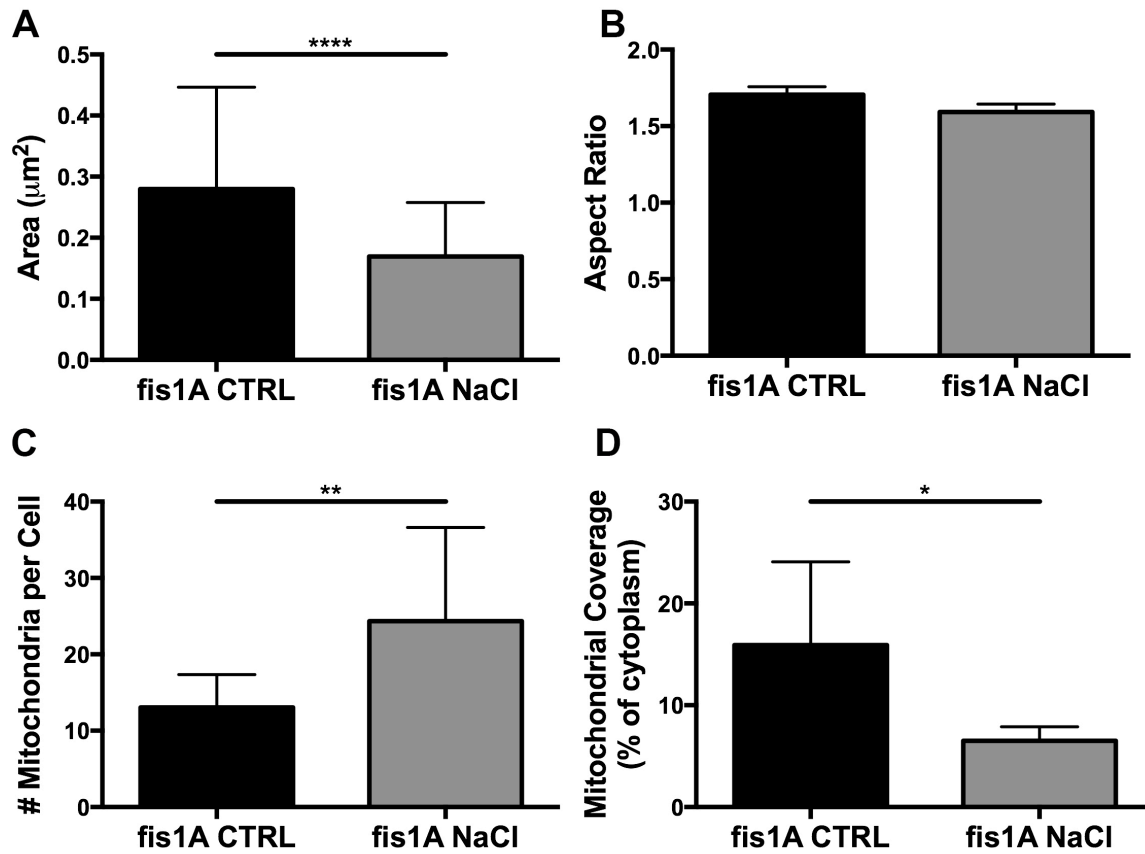


**Figure 18: Comparison of various mitochondrial parameters between *fis1A* mutants under control and salt-stressed conditions.** A) Mitochondrial area, B) Mitochondrial aspect ratio, C) # of mitochondria per cell, D) Mitochondrial coverage as a % of cytoplasm. Statistical analysis indicates significant differences (\*\*\*\*,  $P \leq 0.0001$ , \*\*,  $P \leq 0.01$ , \*,  $P \leq 0.05$ ) compared with controls using one-way ANOVA.

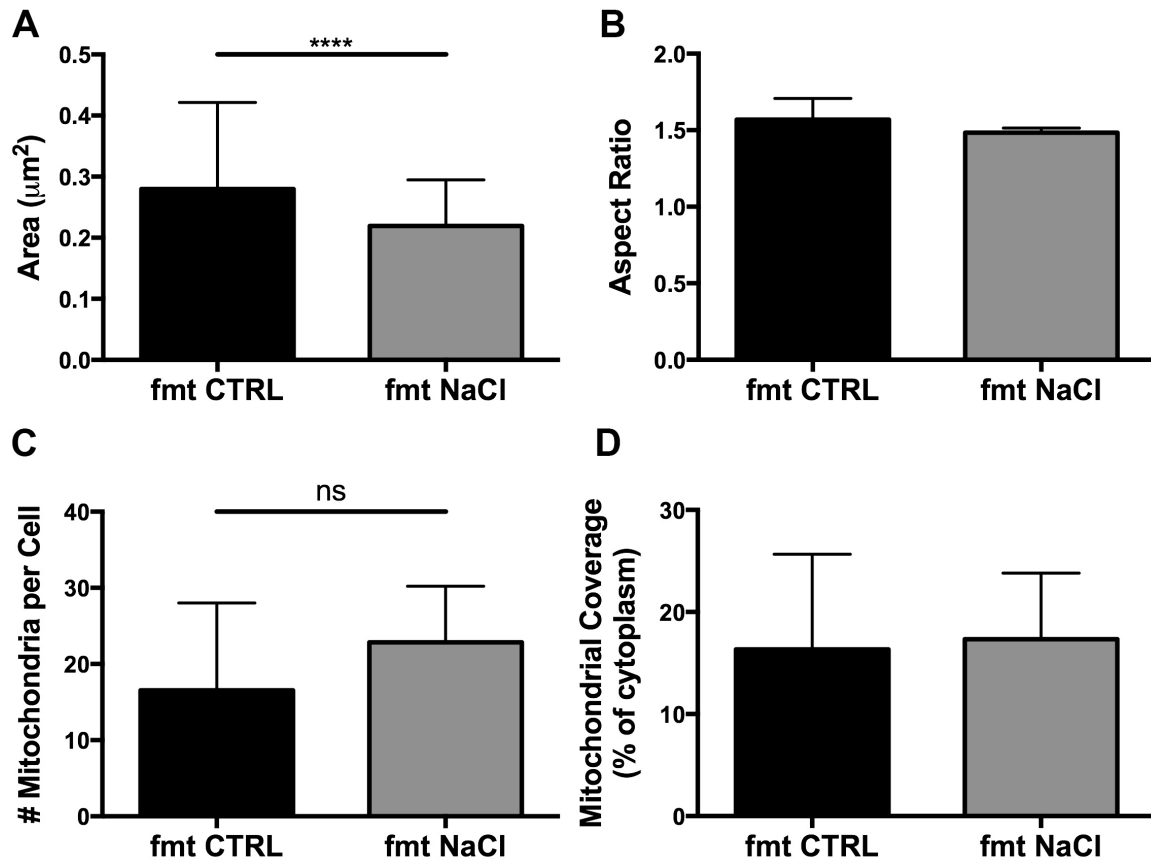


**Figure 19: Comparison of various mitochondrial parameters between *fmt* mutants under control and salt-stressed conditions.** A) Mitochondrial area, B) Mitochondrial aspect ratio, C) # of mitochondria per cell, D) Mitochondrial coverage as a % of cytoplasm. Statistical analysis indicates significant differences (\*\*\*\*,  $P \leq 0.0001$ , ns = not significant,  $P > 0.05$ ) compared with controls using one-way ANOVA.

### 3.5.2 Clustering is regulated by FMT and is sensitive to salt stress

Mutants with a non-functional *CLU* gene show a significant increase in mitochondrial clustering in a variety of species, including slime mold, yeast, and fruit flies (Fields et al., 1998, Cox & Spradling, 2009, Gao et al., 2014). In *Arabidopsis*, it was previously shown via electron microscopy that *fmt* mutants had increased mitochondrial clustering in their leaves (El Zawily et al., 2014), but an analysis of clustering in the roots of *fmt* mutants had yet to be done. Additionally, a similar analysis in *fis1A* and *FMT-OE* plants, as well as an examination of the effects of clustering under salt-stressed conditions was lacking.

We therefore examined mitochondrial clustering in the roots of WT, *fis1A*, *fmt*, and *FMT-OE* plants under control conditions. Due to difficulties in fixing and embedding salt-stressed *FMT-OE* roots, we were only able to analyze the roots of WT, *fis1A*, and *fmt* plants under salt-stressed conditions. We examined mitochondrial clustering using the average nearest neighbor ratio (ANN) (see Materials and Methods). If the average ANN is less than 1, the mitochondria trend towards clustering. If the ANN is greater than 1, the mitochondria trend towards dispersion. We found that indeed, mitochondrial clustering was evident in *fmt* mutants (average  $0.734 \pm 0.617$ ) compared to WT plants ( $1.95 \pm 1.85$ ). Interestingly, both *fis1A* and *FMT-OE* mutants exhibited similar random clustering patterns, with an ANN around 1 ( $1.08 \pm 0.75$ , and  $1.06 \pm 0.752$ , respectively) (Fig. 20A). An analysis of mitochondrial clustering under salt-stressed conditions revealed that WT plants had a decreased ANN ( $0.71 \pm 0.41$ ) compared to WT plants under control conditions, indicating a trend towards mitochondrial clustering under salt stress (Fig. 20B). However, there were no differences in ANN observed in *fis1A* ( $0.95 \pm 0.70$ ) or *fmt* mutant plants ( $0.72 \pm 0.44$ ) (Fig. 20C,D) under salt stress conditions compared to controls.

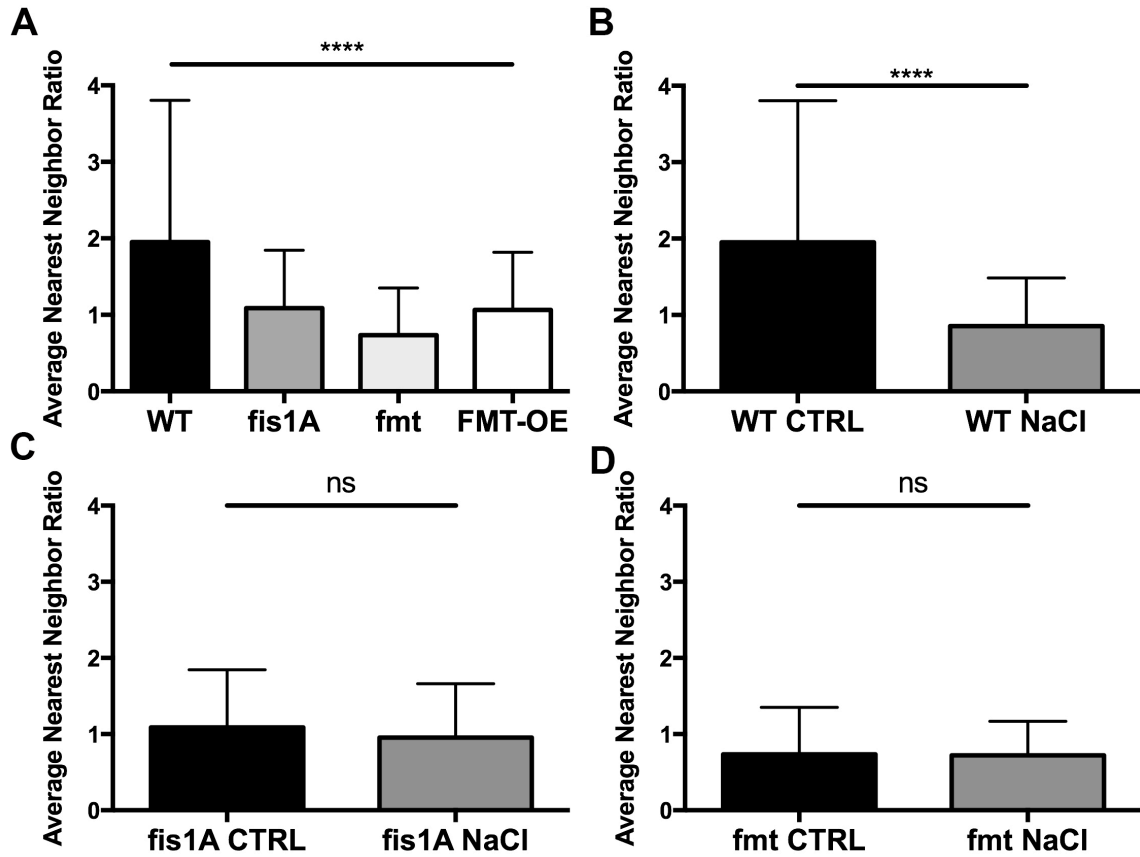


**Figure 20: Clustering patterns in WT, *fis1A*, *fmt*, and *FMT-OE* lines under control and salt-stressed conditions.** A) Clustering as measured by Average Nearest Neighbor ratio (ANN), B) ANN comparison between WT under control and salt-stressed conditions, C) ANN comparison between *fis1A* under control and salt-stressed conditions, D) ANN comparison between *fmt* under control and salt-stressed conditions. Statistical analysis indicates significant differences (\*\*\*\*,  $P \leq 0.0001$ , ns = not significant,  $P > 0.05$ ) compared with controls using one-way ANOVA.

## 4. Discussion

Mitochondria are dynamic organelles that orchestrate a variety of cellular functions in all eukaryotic organisms. Although mitochondria from plants and animals have evolved to suit the particular needs of the organism, some mitochondrial genes remain highly conserved, including *CLU/FMT*, and *FISIA*. The high degree of conservation between these genes across organisms indicates highly conserved and fundamentally important functions. Investigation of these genes in lower organisms such as *Arabidopsis* can help to serve as a simplified model of gene function, which can help to more quickly elucidate function in higher organisms. The function of *CLU* remains unknown, and while the basic function of *FISIA* in mitochondrial fission is known, it is not well understood how these genes function in response to stress. Thus, in order to gain further insight into the function of these genes and how they regulate mitochondrial and whole-plant morphology in response to stress, we performed phenotypic and cellular analyses of *FMT* and *FISIA* in *Arabidopsis* under both control and salt-stressed conditions.

### 4.1 FMT regulates multiple cellular processes in a variety of organisms

*FMT* in *Arabidopsis* belongs to the *CLU* (CLUstered mitochondria) family of genes that is highly conserved throughout eukaryotes, including yeast, fruit flies, and humans (Fields et al., 1998, Cox & Spradling, 2009, Gao et al., 2014). Knockouts of this gene consistently display a phenotype of mitochondrial clustering, leading to the hypothesis that this gene was involved in mitochondrial positioning/orientation within the cell. However, recent work by Gao et al. (2014) revealed that *CLU* may in fact function as an

RNA-binding protein (RBP) that specifically binds mRNAs of nuclear-encoded mitochondrial proteins. CLU may also specifically bind ribosomes on the surface of the mitochondrial outer membrane, in order to help facilitate site-specific mRNA translation (Sen & Cox, 2016). It was also shown that CLU binds TOM20, one component of the TOM mitochondrial import complex that is important for the import of proteins into mitochondria. Additionally, Sen et al. (2015) found that CLU may work to negatively regulate the interaction between PINK1 and PARKIN in *Drosophila*, which has implications for a role in mitochondrial quality control. In this model, under control conditions, PINK1 is normally imported into the mitochondrial inner membrane where it is degraded by PARL, a rhomboid protease. Under conditions of mitochondrial membrane depolarization, mitochondrial protein import is halted, and as a result PINK1 is unable to enter mitochondria. Instead, PINK1 accumulates on the outer mitochondrial membrane, where it is hypothesized to complex with CLU and well as PARKIN. PARKIN then targets the depolarized mitochondrion for ubiquitination and subsequent degradation. This pathway is an example of a quality control mechanism employed by the cell to prevent unhealthy (i.e. depolarized) mitochondria from accumulating within the cytoplasm. Although *Arabidopsis* does not possess homologues for PINK1 or PARKIN, it seems likely that a type of mitochondrial quality control might exist within plants, and may be mediated by FMT. Plants also possess a TOM20 complex on the mitochondrial outer membrane, as well as ubiquitinating enzymes (Duncan et al., 2013). It is therefore not unreasonable to hypothesize that plants may also possess a mechanism for mitochondrial quality control that is mediated by FMT functioning as an RBP.

It was also recently found that the homologue of CLU in humans, CLUH, might serve a function in the localization of nuclear proteins. Ando et al. (2016) showed that CLUH can bind viral influenza M1 proteins and transport them into the nucleus, where viral progeny synthesis and subsequent nuclear export occur. This indicates that CLUH is, in certain cases, able to bring proteins into the nucleus in a manner that can alter transcription. All of these experiments indicate that CLU has evolved to regulate multiple cellular processes in a variety of organisms. However, it is currently unclear whether CLU performs a similar function in *Arabidopsis*, or if it evolved these functions only in higher organisms. Analysis of FMT in *Arabidopsis* by El Zawily et al. (2014) revealed that *fmt* mutants had an increased time of association between mitochondria, as well as increase in matrix mixing between mitochondria, and an increase in the number of transient changes in mitochondrial membrane potential. The authors take these data to indicate deficits in mitochondrial fusion, and imply that FMT may function as a mitochondrial fusion protein. As *Arabidopsis* lacks any homologues to known mitochondrial fusion proteins, it is possible that FMT may serve this function, and in higher organisms this function was eventually relegated to other proteins. Mitochondrial fusion mutants, such as those observed in yeast, worms, and flies (for review see Westermann, 2010), show an increased number of mitochondria, and an increase in numbers of fragmented mitochondria. Although an increase in fragmented mitochondria was not observed in *fmt* mutants in *Arabidopsis*, these mutants did show an increase in mitochondrial number. This supports the claim that FMT may function as a fusion protein in *Arabidopsis*, but more evidence is needed. It is also possible that FMT is not a fusion protein itself, but in fact regulates some as-yet unknown fusion proteins via

mRNA binding. It may also function by negatively regulating the binding of fission proteins to the mitochondrial outer membrane, thereby promoting fusion.

However, considering how similar the phenotypes are between *fmt* mutants in *Arabidopsis* and higher organisms, and the fact that sequence similarity is highly conserved, especially the TPR domain, which was shown to be the RNA binding domain of CLU in *Drosophila*, it seems more likely that FMT and CLU possess similar functions, including RNA binding, and possible tethering to the ribosome and mediation of protein import into mitochondria. Additionally, the role of CLUH in influenza subnuclear transport indicates a role for FMT during stress. Biotic stress of plants, including infection by viruses or bacteria, can induce a variety of responses involving mitochondria (see Introduction). Thus, it is not unreasonable to posit a role for CLU in the biotic stress response in *Arabidopsis*, as well as abiotic stress responses, including salt stress.

#### **4.2 *fmt* and *FMT-OE* mutants show deficits in root and leaf length, and delays in flowering and germination**

El Zawily et al. (2014) observed that *fmt* mutants in *Arabidopsis* displayed shortened roots, an observation that was corroborated by our findings. Additionally, we also found that *fmt* mutants had shorter leaves, as well as increase in the number of days to flowering. Overexpression of FMT in *Arabidopsis* resulted in a significant deficit in percent germination and days to germination, as well as a decrease in leaf length. Roots of *FMT-OE* plants were initially shorter by day 7, but by day 14 had grown to lengths comparable to that of the WT, indicating a key role of FMT in regulating root growth.

The significant delay in germination and flowering in *FMT-OE* and *fmt* mutants, respectively, also indicates a clear role for this gene in both of these processes.

#### **4.2.1 Putative role of FMT in germination and flowering control in *Arabidopsis***

In plants, the switch from vegetative to reproductive growth triggers flowering, and several pathways are known to be involved in the initiation and regulation of this transition (for review see Blumel et al., 2015). Several NAC transcription factors have been shown to play a key role in flowering (Sablowski & Meyerowitz, 1998), as well as germination (Kim et al., 2008) and stress (Tran et al., 2004, He et al., 2005, Jiang & Deyholos, 2006) in *Arabidopsis*. NTL8 is a NAC transcription factor belonging to the sub-family of NTLs (NTM1-Likes), which are also known to function as membrane-associated transcription factors (MTFs). MTFs remain membrane-bound and dormant until they are activated and transported to the nucleus. This mechanism allows for fast and efficient regulation of gene expression in response to environmental changes. MTFs are known to be activated by regulated ubiquitin (Ub)/proteasome-dependent processing (RUP), in which MTFs are ubiquitinated and partially degraded by the 26S proteasome, and subsequently released in transcriptionally active form (Hoppe et al., 2000). NTL8 is unique among other members of the NTL family in that it is highly induced by elevated levels of salt, and an overexpression of NTL8 delays flowering in *Arabidopsis*. It was also found that NTL8 regulates expression of FLOWERING LOCUS T (FT) in salt-responsive flowering (Kim et al., 2007). Additionally, NTL8 was shown to modulate gibberellic acid (GA)-mediated salt signalling during seed germination (Kim et al., 2008). Interestingly, *fmt* mutants display a similar delay in flowering, although not as severe as

*ntl8* mutants. Additionally, *FMT* was shown to be upregulated during salt exposure (Fig. 2). Furthermore, *CLU* was shown to negatively regulate the interaction between *PINK1* and *PARKIN*, (Sen et al., 2015), and *PARKIN* is known to activate a ubiquitin-proteasome system which targets proteins for degradation by recruitment of the 26S proteasome (Aguileta et al., 2015, Um et al., 2010, Livnat-Levanon & Glickman, 2011). Additionally, *CLUH* was shown to bind viral M1 proteins and transport them into the nucleus in a manner that can alter transcription. Thus, it is possible that *FMT* may be able to regulate germination or flowering by mediating *RUP* and subsequent activation of transcription factors that control these processes.

#### **4.3 Changes in *FMT* expression affect mitochondrial size, number, and clustering in columella cells**

In order to gain a more complete understanding of how *FMT* mediates mitochondrial morphology in the roots of *Arabidopsis*, transmission electron microscopy (TEM) analysis was performed in columella cells. Mitochondria in *fmt* mutants were not significantly different in area compared to WT plants, however they had a significantly increased number of mitochondria per cell, leading to increased mitochondrial coverage. As expected, these cells also exhibited significant mitochondrial clustering, consistent with TEM experiments performed in other species and in the leaves of *fmt Arabidopsis* mutants (El Zawily et al., 2014, Cox & Spradling, 2009). TEM analysis of mitochondrial morphology in *FMT-OE* mutants revealed phenotypes opposite to those observed in *fmt* mutants. *FMT-OE* mutants displayed a random clustering pattern and also had fewer numbers of mitochondria compared to *fmt* mutants, and as a result lower mitochondrial

coverage, although these values were not significantly different from the WT. These data provide evidence for FMT in the regulation of mitochondria size, number, and positioning of columella cells in *Arabidopsis* roots. The absence of a “severe” phenotype in *FMT-OE* mutants compared to *fmt* mutants could be explained by the data suggesting that FMT functions as an RBP. It is possible that excess FMT does not have enough ribosomes to bind, and overexpression reaches a certain “threshold” after which point excess FMT has little effect.

#### **4.4 *fis1A* mutants have shorter roots and may regulate mitochondrial clustering**

Mitochondrial fission is essential for cell survival; if a build-up of deleterious components, such as mutated mtDNA, accumulates inside the organelle, it can be segregated to one side and the mitochondrion can divide, leaving one healthy organelle and one bound for autophagy (Youle & van der Bliek, 2012). Mammals and yeast contain only one FIS1 protein, whereas the *Arabidopsis* FIS1 family (AtFIS1) contains two isoforms, FIS1A and FIS1B, which are known to facilitate the division of both mitochondria and peroxisomes (Zhang & Hu, 2008). It was shown that both *fis1A* and *fis1B* single mutants displayed a decrease in the number of peroxisomes and mitochondria. The *fis1A/fis1B* double mutant showed a similar phenotype to the *fis1A* single mutant, with an increase in the incidence of clumped mitochondria and peroxisomes, as well as a significant increase in size and number of the two organelles, indicating a deficit in fission. However, the total organelle volume was slightly lower in the double mutants than in the *fis1A* single mutant, indicating that these two proteins may have overlapping or redundant functions. Overexpression of either FIS1A or FIS1B

increased the abundance of both mitochondria and peroxisomes, but no obvious physiological changes were observed (Zhang & Hu, 2008). While this preliminary research helped to determine that *Arabidopsis* FIS1 proteins have a similar role to their mammalian and yeast counterparts, an examination of these proteins in the roots, as well as under salt-stressed conditions, had yet to be done. Since FIS1A and FIS1B were shown to have partially redundant roles, and since the *fis1A/fis1B* double mutant was unavailable, we decided to examine the *fis1A* mutant in *Arabidopsis* roots, under both control and salt-stressed conditions. The most significant phenotype of *fis1A* mutants was significantly shorter roots, but all other phenotypic characteristics measured did not vary significantly from the WT. Thus, FIS1A may regulate root length, possibly through a control of mitochondrial fission. Interestingly, *fis1A* mutants did not display a decrease in numbers of mitochondria, or an increase in area, as was previously described (Scott et al., 2006, Zhang & Hu, 2008). This can be explained by differences in technique; previous experiments were done in leaves, while we examined mitochondria in the roots. In addition, mitochondria were visualized using a fluorescence-tagged protein under low magnification, while we used high-resolution electron microscopy. As a result, while a cluster of fluorescently tagged mitochondria may appear as a large clump and may be counted as a single mitochondrion, using our technique we were able to discern individual mitochondria within in a single cell, and thus gain a more accurate representation of mitochondrial number and size, as well as various other mitochondrial parameters not possible with previous techniques. Although we did not see significant differences in mitochondrial size, AR, or number, we did see an increase in mitochondrial coverage. This could be due to a decrease in overall cell size, and thus a decrease in total

cytoplasm, although this was not quantified. It is important to note that the FIS1B isoform is still functional in *fis1A* mutants, meaning that mitochondrial fission is not totally abolished. While previous research suggested that *fis1A/fis1B* double mutants have similar phenotypes to *fis1A* single mutants, it appears that this is not the case on the level of individual mitochondrial morphology. However, *fis1A* mutants did display a tendency towards “random” clustering, as opposed to dispersion, as was observed in the WT. Thus, it appears that FIS1A may have a functional role in controlling mitochondrial clustering, likely through control of fission, in columella cells in *Arabidopsis* roots.

#### **4.5 Salt stress affects various phenotypic and mitochondrial parameters**

While it is well established that salt stress has adverse effects in plants, an analysis of the changes to mitochondrial morphology in response to salt stress had yet to be done. Additionally, analyses of various phenotypic and mitochondrial parameters in *fmt* and *fis1A* mutants exposed to salt-stress was lacking. Salt stress is first sensed in the root, and salt-stress-coping mechanisms, such as salt-avoidance tropism, are known to involve the root cap. Additionally, mitochondria are known to play a key role in the salt stress response. As such, we performed an analysis of phenotypic and mitochondrial morphology in the *Arabidopsis* root in WT, *fmt*, and *fis1A* mutants under salt-stressed conditions.

Upon exposure to salt stress, WT plants exhibited a decrease in root and leaf length, as well as an increase in days to germination and time to flowering. These same changes were observed in *fis1A* mutants. *fmt* mutants exhibited significantly shorter roots compared to WT plants under control conditions. Leaf length was shorter compared to

WT plants under salt stress, but not compared to *fmt* mutants under control conditions. Interestingly, there was no increase in days to flowering, as was seen in WT, *fis1A*, and *FMT-OE* plants under the same salt stress conditions. In contrast, salt stress further exacerbated the decreased germination rate and time to germination of *FMT-OE* plants. Additionally, these plants exhibited an increase in days to flowering and decreases in root and leaf length.

These data indicate that salt stress affects all major phenotypic parameters in *Arabidopsis* wild type plants, although percent germination was unaffected. However, salt inhibition of seed germination (SSG) is a well-known phenomenon (Lee et al., 2010, Yu et al., 2016), although it is usually known to occur under conditions of high salinity (>150mM NaCl). It is therefore likely that we would see an inhibition of germination if our experiments were repeated at a higher level of salt exposure. The exacerbation of the *FMT-OE* germination suppression phenotypes following salt exposure further implicates this gene in regulation of germination, especially during salt stress. Interestingly, despite the fact that *fmt* mutants displayed an increase in days to flowering under control conditions, this phenotype was not exacerbated upon exposure to salt stress. In addition, root and leaf length were not significantly increased in *fmt* mutants under salt-stressed conditions. These data indicate that salt stress-induced changes, such as an increase in days to flowering and a decrease in leaf and root length, as were observed in the WT, are, at least in part, under the control of *FMT*.

An observation of the mitochondria of salt-stressed wild type plants under the electron microscope revealed a decrease in mitochondrial area as well as an increase in mitochondrial number and coverage. A tendency towards clustering was also observed.

*fmt* mutants displayed a decrease in mitochondrial area while AR, mitochondrial number, coverage, and clustering remained unchanged. *fis1A* mutant plants displayed a decrease in mitochondrial area and coverage, with an increase in mitochondrial number, while clustering and AR were not significantly different.

These data further implicate mitochondria in the salt stress response, as it is clear they undergo dynamic changes upon exposure to NaCl. The dynamic increase in number and decrease in size indicates an increased demand for these organelles, possibly through an upregulation of fission. Additionally, these data indicate that mitochondrial number and clustering may be regulated by FMT and FIS1A during NaCl stress.

#### **4.6 Conclusion and future perspectives**

This study has provided several insights into the roles of the *FMT* and *FIS1A* genes in whole-plant and mitochondrial morphology. It was found that *FMT* may work to regulate root and leaf length, as well as flowering, under both control and salt-stressed conditions. It was also found that *FMT* controls mitochondrial organization via clustering, as well as mitochondrial number under both control and salt-stressed conditions. *FIS1A* was found to potentially regulate root length as well as mitochondrial clustering. Salt stress was also found to affect various mitochondrial parameters, including mitochondrial area, number, and clustering.

More work must be done to fully characterize FMT and FIS1A under both control and salt-stressed conditions. Future research will focus on elucidating the mechanisms of fission in root length control as well as clustering. It appears that CLU may function as an RNA-binding protein in other species, and it should be seen if this is also true for FMT

in *Arabidopsis*. The role of FMT in salt-avoidance tropism and amyloplast degradation should also be examined. Putative targets of FMT, such as NTL8 and PIN2, and potential ubiquitination of these proteins, should also be explored.

## References

1. Aguilera MA, Korac J, Durcan TM, *et al.*, 2015. The E3 ubiquitin ligase parkin is recruited to the 26 S proteasome via the proteasomal ubiquitin receptor Rpn13. *J Biol Chem* **290**, 7492-505.
2. Ando T, Yamayoshi S, Tomita Y, Watanabe S, Watanabe T, Kawaoka Y, 2016. The host protein CLUH participates in the subnuclear transport of influenza virus ribonucleoprotein complexes. *Nature Microbiology*, 16062.
3. Andronis EA, Roubelakis-Angelakis KA, 2010. Short-term salinity stress in tobacco plants leads to the onset of animal-like PCD hallmarks in planta in contrast to long-term stress. *Planta* **231**, 437-48.
4. Aung K, Hu J, 2012. Differential roles of Arabidopsis dynamin-related proteins DRP3A, DRP3B, and DRP5B in organelle division. *J Integr Plant Biol* **54**, 921-31.
5. Barrada A, Montane MH, Robaglia C, Menand B, 2015. Spatial Regulation of Root Growth: Placing the Plant TOR Pathway in a Developmental Perspective. *Int J Mol Sci* **16**, 19671-97.
6. Blumel M, Dally N, Jung C, 2015. Flowering time regulation in crops-what did we learn from Arabidopsis? *Curr Opin Biotechnol* **32**, 121-9.
7. Cardon GE, 2007. *Managing saline soils*. Colorado State University Cooperative Extension.
8. Carillo P, Annunziata MG, Pontecorvo G, Fuggi A, Woodrow P, 2011. Salinity stress and salt tolerance. *Abiotic Stress Plants-Mech. Adapt.*

9. Chen H, Chan DC, 2009. Mitochondrial dynamics--fusion, fission, movement, and mitophagy--in neurodegenerative diseases. *Hum Mol Genet* **18**, R169-76.
10. Clark PJ, Evans FC, 1954. Distance to nearest neighbor as a measure of spatial relationships in populations. *Ecology* **35**, 445-53.
11. Clough SJ, Bent AF, 1998. Floral dip: a simplified method for Agrobacterium-mediated transformation of *Arabidopsis thaliana*. *Plant J* **16**, 735-43.
12. Conti L, Price G, O'donnell E, Schwessinger B, Dominy P, Sadanandom A, 2008. Small ubiquitin-like modifier proteases OVERLY TOLERANT TO SALT1 and 2 regulate salt stress responses in *Arabidopsis*. *Plant Cell* **20**, 2894-908.
13. Cox RT, Spradling AC, 2009. Clueless, a conserved *Drosophila* gene required for mitochondrial subcellular localization, interacts genetically with parkin. *Dis Model Mech* **2**, 490-9.
14. De Dorlodot S, Forster B, Pages L, Price A, Tuberosa R, Draye X, 2007. Root system architecture: opportunities and constraints for genetic improvement of crops. *Trends Plant Sci* **12**, 474-81.
15. Duan L, Sebastian J, Dinneny JR, 2015. Salt-stress regulation of root system growth and architecture in *Arabidopsis* seedlings. *Methods Mol Biol* **1242**, 105-22.
16. Duncan O, Murcha MW, Whelan J, 2013. Unique components of the plant mitochondrial protein import apparatus. *Biochim Biophys Acta* **1833**, 304-13.
17. El Zawily AM, Schwarzlander M, Finkemeier I, *et al.*, 2014. FRIENDLY regulates mitochondrial distribution, fusion, and quality control in *Arabidopsis*. *Plant Physiol* **166**, 808-28.

18. Fields SD, Conrad MN, Clarke M, 1998. The *S. cerevisiae* CLU1 and D. discoideum cluA genes are functional homologues that influence mitochondrial morphology and distribution. *J Cell Sci* **111** ( Pt 12), 1717-27.
19. Gao C, Xing D, Li L, Zhang L, 2008. Implication of reactive oxygen species and mitochondrial dysfunction in the early stages of plant programmed cell death induced by ultraviolet-C overexposure. *Planta* **227**, 755-67.
20. Gao J, Schatton D, Martinelli P, *et al.*, 2014. CLUH regulates mitochondrial biogenesis by binding mRNAs of nuclear-encoded mitochondrial proteins. *J Cell Biol* **207**, 213-23.
21. Hasegawa PM, Bressan RA, Zhu JK, Bohnert HJ, 2000. Plant Cellular and Molecular Responses to High Salinity. *Annu Rev Plant Physiol Plant Mol Biol* **51**, 463-99.
22. Hauser F, Horie T, 2010. A conserved primary salt tolerance mechanism mediated by HKT transporters: a mechanism for sodium exclusion and maintenance of high K(+)/Na(+) ratio in leaves during salinity stress. *Plant Cell Environ* **33**, 552-65.
23. He XJ, Mu RL, Cao WH, Zhang ZG, Zhang JS, Chen SY, 2005. AtNAC2, a transcription factor downstream of ethylene and auxin signaling pathways, is involved in salt stress response and lateral root development. *Plant J* **44**, 903-16.
24. Heath MC, 2000. Hypersensitive response-related death. *Plant Mol Biol* **44**, 321-34.
25. Hoppe T, Matuschewski K, Rape M, Schlenker S, Ulrich HD, Jentsch S, 2000. Activation of a membrane-bound transcription factor by regulated ubiquitin/proteasome-dependent processing. *Cell* **102**, 577-86.

26. James DI, Parone PA, Mattenberger Y, Martinou JC, 2003. hFis1, a novel component of the mammalian mitochondrial fission machinery. *J Biol Chem* **278**, 36373-9.
27. Ji H, Pardo JM, Batelli G, Van Oosten MJ, Bressan RA, Li X, 2013. The Salt Overly Sensitive (SOS) pathway: established and emerging roles. *Mol Plant* **6**, 275-86.
28. Jiang Y, Deyholos MK, 2006. Comprehensive transcriptional profiling of NaCl-stressed Arabidopsis roots reveals novel classes of responsive genes. *BMC Plant Biol* **6**, 25.
29. Jones B, Ljung K, 2012. Subterranean space exploration: the development of root system architecture. *Curr Opin Plant Biol* **15**, 97-102.
30. Kim SG, Kim SY, Park CM, 2007. A membrane-associated NAC transcription factor regulates salt-responsive flowering via FLOWERING LOCUS T in Arabidopsis. *Planta* **226**, 647-54.
31. Kim SG, Lee AK, Yoon HK, Park CM, 2008. A membrane-bound NAC transcription factor NTL8 regulates gibberellic acid-mediated salt signaling in Arabidopsis seed germination. *Plant J* **55**, 77-88.
32. Lam E, Kato N, Lawton M, 2001. Programmed cell death, mitochondria and the plant hypersensitive response. *Nature* **411**, 848-53.
33. Lee S, Kim SG, Park CM, 2010. Salicylic acid promotes seed germination under high salinity by modulating antioxidant activity in Arabidopsis. *New Phytol* **188**, 626-37.

34. Livnat-Levanon N, Glickman MH, 2011. Ubiquitin-proteasome system and mitochondria - reciprocity. *Biochim Biophys Acta* **1809**, 80-7.
35. Logan DC, 2010. Mitochondrial fusion, division and positioning in plants. *Biochem Soc Trans* **38**, 789-95.
36. Logan DC, Scott I, Tobin AK, 2003. The genetic control of plant mitochondrial morphology and dynamics. *Plant J* **36**, 500-9.
37. Malamy JE, 2005. Intrinsic and environmental response pathways that regulate root system architecture. *Plant Cell Environ* **28**, 67-77.
38. Malekpoor Mansoorkhani F, Seymour GB, Swarup R, Moeiniyan Bagheri H, Ramsey RJ, Thompson AJ, 2014. Environmental, developmental, and genetic factors controlling root system architecture. *Biotechnol Genet Eng Rev* **30**, 95-112.
39. Mitchell A, 2005. The ESRI guide to GIS analysis, Volume 2: Spatial Measurements and Statistics. Redlands. In.: CA: Esri Press.
40. Miyagishima SY, Kuwayama H, Urushihara H, Nakanishi H, 2008. Evolutionary linkage between eukaryotic cytokinesis and chloroplast division by dynamin proteins. *Proc Natl Acad Sci U S A* **105**, 15202-7.
41. Morel JB, Dangl JL, 1997. The hypersensitive response and the induction of cell death in plants. *Cell Death Differ* **4**, 671-83.
42. Mozdy AD, Mccaffery JM, Shaw JM, 2000. Dnm1p GTPase-mediated mitochondrial fission is a multi-step process requiring the novel integral membrane component Fis1p. *J Cell Biol* **151**, 367-80.

43. Munns R, Tester M, 2008. Mechanisms of salinity tolerance. *Annu Rev Plant Biol* **59**, 651-81.
44. Nunnari J, Suomalainen A, 2012. Mitochondria: in sickness and in health. *Cell* **148**, 1145-59.
45. Ottenschlager I, Wolff P, Wolverton C, *et al.*, 2003. Gravity-regulated differential auxin transport from columella to lateral root cap cells. *Proc Natl Acad Sci U S A* **100**, 2987-91.
46. Pitman MG, Läuchli A, 2002. Global Impact of Salinity and Agricultural Ecosystems. In: Läuchli A, Lüttge U, eds. *Salinity: Environment - Plants - Molecules*. Dordrecht: Springer Netherlands, 3-20.
47. Praefcke GJ, McMahon HT, 2004. The dynamin superfamily: universal membrane tubulation and fission molecules? *Nat Rev Mol Cell Biol* **5**, 133-47.
48. Rosado A, Schapire AL, Bressan RA, *et al.*, 2006. The Arabidopsis tetratricopeptide repeat-containing protein TTL1 is required for osmotic stress responses and abscisic acid sensitivity. *Plant Physiol* **142**, 1113-26.
49. Sablowski RW, Meyerowitz EM, 1998. A homolog of NO APICAL MERISTEM is an immediate target of the floral homeotic genes APETALA3/PISTILLATA. *Cell* **92**, 93-103.
50. Sato EM, Hijazi H, Bennett MJ, Vissenberg K, Swarup R, 2015. New insights into root gravitropic signalling. *J Exp Bot* **66**, 2155-65.
51. Scott I, Logan DC, 2008. Mitochondria and cell death pathways in plants: Actions speak louder than words. *Plant Signal Behav* **3**, 475-7.

52. Scott I, Tobin AK, Logan DC, 2006. BIGYIN, an orthologue of human and yeast FIS1 genes functions in the control of mitochondrial size and number in *Arabidopsis thaliana*. *J Exp Bot* **57**, 1275-80.
53. Sen A, Cox RT, 2016. Clueless is a conserved ribonucleoprotein that binds the ribosome at the mitochondrial outer membrane. *Biol Open* **5**, 195-203.
54. Sen A, Kalvakuri S, Bodmer R, Cox RT, 2015. Clueless, a protein required for mitochondrial function, interacts with the PINK1-Parkin complex in *Drosophila*. *Dis Model Mech* **8**, 577-89.
55. Shimada TL, Shimada T, Hara-Nishimura I, 2010. A rapid and non-destructive screenable marker, FAST, for identifying transformed seeds of *Arabidopsis thaliana*. *Plant J* **61**, 519-28.
56. Smirnova E, Griparic L, Shurland DL, Van Der Bliet AM, 2001. Dynamin-related protein Drp1 is required for mitochondrial division in mammalian cells. *Mol Biol Cell* **12**, 2245-56.
57. Srivastava AK, Zhang C, Sadanandom A, 2016. Rice OVERLY TOLERANT TO SALT 1 (OTS1) SUMO protease is a positive regulator of seed germination and root development. *Plant Signal Behav* **11**, e1173301.
58. Sun F, Zhang W, Hu H, *et al.*, 2008. Salt modulates gravity signaling pathway to regulate growth direction of primary roots in *Arabidopsis*. *Plant Physiol* **146**, 178-88.
59. Tieu Q, Nunnari J, 2000. Mdv1p is a WD repeat protein that interacts with the dynamin-related GTPase, Dnm1p, to trigger mitochondrial division. *J Cell Biol* **151**, 353-66.

60. Tran LS, Nakashima K, Sakuma Y, *et al.*, 2004. Isolation and functional analysis of Arabidopsis stress-inducible NAC transcription factors that bind to a drought-responsive cis-element in the early responsive to dehydration stress 1 promoter. *Plant Cell* **16**, 2481-98.
61. Um JW, Im E, Lee HJ, *et al.*, 2010. Parkin directly modulates 26S proteasome activity. *J Neurosci* **30**, 11805-14.
62. Van Der Merwe MJ, Osorio S, Moritz T, Nunes-Nesi A, Fernie AR, 2009. Decreased mitochondrial activities of malate dehydrogenase and fumarase in tomato lead to altered root growth and architecture via diverse mechanisms. *Plant Physiol* **149**, 653-69.
63. Vandecasteele G, Szabadkai G, Rizzuto R, 2001. Mitochondrial calcium homeostasis: mechanisms and molecules. *IUBMB Life* **52**, 213-9.
64. Vellosillo T, Aguilera V, Marcos R, *et al.*, 2013. Defense activated by 9-lipoxygenase-derived oxylipins requires specific mitochondrial proteins. *Plant Physiol* **161**, 617-27.
65. Wang Y, Zhang W, Li K, *et al.*, 2008. Salt-induced plasticity of root hair development is caused by ion disequilibrium in Arabidopsis thaliana. *J Plant Res* **121**, 87-96.
66. Westermann B, 2010. Mitochondrial dynamics in model organisms: what yeasts, worms and flies have taught us about fusion and fission of mitochondria. *Semin Cell Dev Biol* **21**, 542-9.

67. Wu S, Baskin TI, Gallagher KL, 2012. Mechanical fixation techniques for processing and orienting delicate samples, such as the root of *Arabidopsis thaliana*, for light or electron microscopy. *Nat Protoc* **7**, 1113-24.
68. Wu SJ, Ding L, Zhu JK, 1996. SOS1, a Genetic Locus Essential for Salt Tolerance and Potassium Acquisition. *Plant Cell* **8**, 617-27.
69. Youle RJ, Karbowski M, 2005. Mitochondrial fission in apoptosis. *Nat Rev Mol Cell Biol* **6**, 657-63.
70. Youle RJ, Van Der Bliek AM, 2012. Mitochondrial fission, fusion, and stress. *Science* **337**, 1062-5.
71. Yu Y, Wang J, Shi H, *et al.*, 2016. Salt Stress and Ethylene Antagonistically Regulate Nucleocytoplasmic Partitioning of COP1 to Control Seed Germination. *Plant Physiol* **170**, 2340-50.
72. Zhang L, Xing D, 2008. Methyl jasmonate induces production of reactive oxygen species and alterations in mitochondrial dynamics that precede photosynthetic dysfunction and subsequent cell death. *Plant Cell Physiol* **49**, 1092-111.
73. Zhang M, Wang C, Lin Q, *et al.*, 2015. A tetratricopeptide repeat domain-containing protein SSR1 located in mitochondria is involved in root development and auxin polar transport in *Arabidopsis*. *Plant J* **83**, 582-99.
74. Zhang XC, Hu JP, 2008. FISSION1A and FISSION1B proteins mediate the fission of peroxisomes and mitochondria in *Arabidopsis*. *Mol Plant* **1**, 1036-47.
75. Zhu JK, Liu J, Xiong L, 1998. Genetic analysis of salt tolerance in *Arabidopsis*. Evidence for a critical role of potassium nutrition. *Plant Cell* **10**, 1181-91.

76. Zhu Q, Hulen D, Liu T, Clarke M, 1997. The *cluA*- mutant of *Dictyostelium* identifies a novel class of proteins required for dispersion of mitochondria. *Proc Natl Acad Sci U S A* **94**, 7308-13.
77. Zolla G, Heimer YM, Barak S, 2010. Mild salinity stimulates a stress-induced morphogenic response in *Arabidopsis thaliana* roots. *J Exp Bot* **61**, 211-24.

## **Danksagung**

I would like to thank all of those who supported me throughout my dissertation, and who contributed to the success of this work. I would like to thank my supervisor, Dr. Tamas Horvath, for his continual support and guidance, and constant encouragement of my independent research. I would also like to thank the members of my committee, Dr. Jens Brüning, Dr. Peter Kloppenburg, and Dr. Thomas Langer, for their help and suggestions.

I would like to thank both the University of Cologne and Yale University for providing me with the research tools to help me complete my dissertation.

I would also like to thank my colleagues for providing me with a wonderful work environment, as well as their continued scientific and philosophical input.

Finally, I would like to thank my family, and my partner, for their unyielding love and support in all aspects of my life.

Thank you!

## Erklärung

Köln, 2016

Ich versichere, dass ich die von mir vorgelegte Dissertation selbstständig angefertigt, die benutzten Quellen und Hilfsmittel vollständig angegeben und die Stellen der Arbeit – einschließlich Tabellen, Karten und Abbildungen –, die anderen Werken im Wortlaut oder dem Sinn nach entnommen sind, in jedem Einzelfall als Entlehnung kenntlich gemacht habe; dass diese Dissertation noch keiner anderen Fakultät oder Universität zur Prüfung vorgelegen hat; dass sie – abgesehen von unten angegebenen Teilpublikationen – noch nicht veröffentlicht worden ist sowie, dass ich eine solche Veröffentlichung vor Abschluss des Promotionsverfahrens nicht vornehmen werde. Die Bestimmungen dieser Promotionsordnung sind mir bekannt. Die von mir vorgelegte Dissertation ist von Dr. Prof. Jens Brüning und Dr. Prof. Peter Kloppenburg betreut worden.

---

Alexandra Ralevski

## Lebenslauf

**Name** Alexandra Ralevski  
**Email** alexandra.ralevski@yale.edu  
**Geburtstag** 10.05.1988  
**Geburtsort** Toronto, ON, Canada

## Ausbildung

*2006* Abitur

*2006 – 2010* Studium an der McGill Universität auf Montréal,  
Diplomstudiengang Biologie und Genetik

*2010 – 2013* Master-Studium der Concordia Universität auf Montréal,  
Diplomstudiengang Pflanzenbiologie  
Thema: „The Interaction of Early Salt Stress-Induced 2  
(ESI2) and the Ran G Protein in *Arabidopsis*“

*2013-2016* Recherchiert an der Yale University auf New Haven

*2016* Promotion an der Universität zu Köln, Mathematisch-  
Naturwissenschaftliche Fakultät